JOURNAL OF VIROLOGY, Nov. 2006, p. 10683–10691 Vol. 80, No. 21
0022-538X/06/$08.00+0 doi:10.1128/JVI.01009-06

De Novo Human T-Cell Leukemia Virus Type 1 Infection of Human Lymphocytes in NOD-SCID, Common γ-Chain Knockout Mice▽

Paola Miyazato,[1] Jun-ichirou Yasunaga,[1] Yuko Taniguchi,[1] Yoshio Koyanagi,[2] Hiroaki Mitsuya,[3] and Masao Matsuoka[1]*

Laboratory of Virus Immunology[1] and Laboratory of Virus Pathogenesis,[2] Institute for Virus Research, Kyoto University, Kyoto 606-8507, Japan, and Department of Hematology and Department of Infectious Diseases, Graduate School of Medicine, Kumamoto University, Kumamoto 860-8556, Japan[3]

Received 17 May 2006/Accepted 21 August 2006

Human T-cell leukemia virus type 1 (HTLV-1) is the etiologic agent of adult T-cell leukemia, a disease that is triggered after a long latency period. HTLV-1 is known to spread through cell-to-cell contact. In an attempt to study the events in early stages of HTLV-1 infection, we inoculated uninfected human peripheral blood mononuclear cells and the HTLV-1-producing cell line MT-2 into NOD-SCID, common γ-chain knockout mice (human PBMC-NOG mice). HTLV-1 infection was confirmed with the detection of proviral DNA in recovered samples. Both $CD4^+$ and $CD8^+$ T cells were found to harbor the provirus, although the latter population harbored provirus to a lesser extent. Proviral loads increased with time, and inverse PCR analysis revealed the oligoclonal proliferation of infected cells. Although *tax* gene transcription was suppressed in human PBMC-NOG mice, it increased after in vitro culture. This is similar to the phenotype of HTLV-1-infected cells isolated from HTLV-1 carriers. Furthermore, the reverse transcriptase inhibitors azidothymidine and tenofovir blocked primary infection in human PBMC-NOG mice. However, when tenofovir was administered 1 week after infection, the proviral loads did not differ from those of untreated mice, indicating that after initial infection, clonal proliferation of infected cells was predominant over de novo infection of previously uninfected cells. In this study, we demonstrated that the human PBMC-NOG mouse model should be a useful tool in studying the early stages of primary HTLV-1 infection.

Human T-cell leukemia virus type 1 (HTLV-1) was the first retrovirus shown to be related to human diseases (21, 44), including adult T-cell leukemia (ATL) (50, 51, 58) and HTLV-1-associated myelopathy/tropical spastic paraparesis (HAM/TSP) (16, 43). The infectivity of free virions is much lower than that of infected cells: transmission is cell mediated (8). Glucose transporter 1 has been identified as an HTLV-1 receptor (35). After infected cells form virological synapses with uninfected cells, the viral genome is transferred into uninfected cells (23). Hence, a salient feature of HTLV-1 infection is that this virus transmits in a cell-to-cell fashion. After infection, HTLV-1 facilitates cell-to-cell transmission by forcing the proliferation of infected cells via the actions of its accessory genes.

In the early stage of HTLV-1 infection, accessory genes including *p12*, *p30*, *p13*, and *HBZ*, have been reported to be important for in vivo proliferation of infected cells (3, 5, 22, 47). The gene product p12 plays a critical role by releasing calcium from the endoplasmic reticulum to activate nuclear factor of activated T cell-mediated transcription (2). In addition, p12 enhances lymphocyte-associated antigen-1-mediated cell adhesion, which might facilitate cell-to-cell transmission of HTLV-1 (29), and downmodulates the expression of major histocompatibility complex class I antigens (26). p30 has been reported to suppress viral gene transcription by different mechanisms (41). Other functions of p30 have been also demonstrated, such as the enhancement of the transcription of cellular genes associated with cell proliferation (38, 64). In addition, the *tax* gene is believed to play a central role in proliferation of infected cells by its pleiotropic actions (14, 17, 63). On the other hand, Tax-expressing cells are rapidly eliminated in vivo, since the Tax protein is a major target antigen of cytotoxic T lymphocytes (CTLs) (4, 27). In ATL cells, Tax expression has been shown to be suppressed by several mechanisms (52), strongly suggesting that the loss of Tax expression might be advantageous at the stage of leukemia (36). These studies reveal that the host immune system plays an important role in limiting the proliferation of infected cells. During the long latency period that spans decades, this immune pressure selects those clones with enough alterations to become malignant, eventually leading to the development of ATL.

In vivo studies of HTLV-1 infection have been carried out mainly by inoculating virus-producing or HTLV-1-immortalized cell lines into different animal species (32). Rabbits proved to be an effective model for HTLV-1 infection (1, 65). In addition, monkeys and rats have been used to analyze the in vivo proliferation of HTLV-1-infected cells (7, 55). Furthermore, immunodeficient mouse strains were also able to engraft some HTLV-1-immortalized cell lines (13, 24). These animal models are useful for studying the infection or testing therapeutic agents. However, the early steps of primary HTLV-1 infection remain uninvestigated due to the lack of in vivo experiments using human lymphocytes.

The NOD-SCID (nonobese diabetic-severe combined immunodeficiency), common γ-chain knockout (NOG) mouse was shown to be an excellent recipient for transplantation of

* Corresponding author. Mailing address: Laboratory of Virus Immunology, Institute for Virus Research, Kyoto University, Shogoin Kawahara-cho 53, Sakyo-ku, Kyoto 606-8507, Japan. Phone: 81-75-751-4048. Fax: 81-75-751-4049. E-mail: mmatsuok@virus.kyoto-u.ac.jp.

Published ahead of print on 30 August 2006.

human cells due to multiple immune dysfunctions (9, 25, 60). We report here the primary infection of human lymphocytes in this newly developed mouse strain and characterize the infection by measuring proviral load as well as determining the clonality pattern. Furthermore, we tested whether the existing antiretroviral drugs azidothymidine (AZT) and tenofovir blocked primary infection in this mouse model. This small animal model allows us to better understand the mechanism of HTLV-I infection.

MATERIALS AND METHODS

Cells. Peripheral blood mononuclear cells (PBMC) were isolated from healthy blood donors by Ficoll-Paque Plus (Pharmacia, Uppsala, Sweden) density gradient centrifugation. MT-2, an HTLV-I-producing cell line (61), was used as the source of virus in all the experiments. MT-2 cells were treated with 50 μg/ml of mitomycin C (MMC) (Kyowa, Tokyo, Japan) for 30 min at 37°C in RPMI 1640 supplemented with 10% fetal bovine serum and antibiotics and washed four times with culture medium prior to inoculation into mice. PBMC of 14 healthy donors were used in the experiments. For in vitro cytotoxicity assays, PBMC were stimulated with phytohemagglutinin (PHA) (Sigma, St. Louis, Mo.) prior to use.

Mice. The NOG strain of mice, which was generated by backcross matings of C57BL/6J-*scid*^{null} mice and NOD/Shi-SCID mice, is homozygous for the SCID mutation and the interleukin 2Rγ allelic mutation. It was previously reported to present multiple immunological dysfunctions that include the absence of T, B, and NK cells and also impaired activity of dendritic cells (25). Mice were purchased from the Central Institute of Experimental Animals (Kanagawa, Japan) and were maintained in microisolator cages under specific-pathogen-free conditions in the animal facility of the Institute for Virus Research, Kyoto University (Kyoto, Japan). Mice were 6 to 7 weeks old at the time of the human PBMC transfer.

Transplantation of human PBMC in NOG mice and infection with HTLV-I. A total of 10^7 human PBMC were injected intraperitoneally into each mouse, producing chimeric mice, which we will refer to as hu-PBMC-NOG mice. Three days later, the mice were inoculated intraperitoneally with MMC-treated MT-2 cells (10^3 or 10^4 cells/mouse). Spleens and cells obtained from peritoneal lavage were harvested two or four weeks after injection of MT-2 cells. Human mononuclear cells were isolated by Ficoll-Paque Plus (Pharmacia) density gradient centrifugation prior to analysis. The experimental protocol was approved by the Ethics Review Committee for Animal Experimentation of Institute for Virus Research, Kyoto University. In each independent experiment, PBMC from a single donor were used.

Quantification of HTLV-I proviral load. Genomic DNA was obtained from the samples by standard proteinase K treatment. To quantify the proviral load, we performed a real-time PCR as we described previously (62). The primers for exon 3 of the HTLV-I *tax* gene were 5′-GAAGACTGTTTGCCCACCACC-3′ and 5′-TGAGGGTTGAGTGGAACGGA-3′, and the probe was 5′-CACCCG TCACGCTAACAGCCTGGCAA-3′. Genomic DNA (500 ng) was used for real-time PCR in a 50-μl reaction solution prepared with TaqMan Universal PCR master mix (Applied Biosystems, Foster City, CA). The amplification conditions were 50°C for 2 min, 95°C for 10 min, and then 40 cycles of 15 s at 95°C followed by 60 s at 60°C. All experiments were performed and analyzed using the ABI PRISM 7700 sequence detection system (Applied Biosystems). To measure cell equivalents in the input DNA, the recombination activating gene 1 (*RAG-1*) coding sequence in each sample was also quantified by real-time PCR. The sequences of the primers for *RAG-1* exon 2 detection were 5′-CCCACCTTGG GACTCAGTTCT-3′ and 5′-CACCCGGAACAGCTTAAATTTC-3′, and the probe was 5′-CCCCAGATGAAATTCAGCACCCACATA-3′. Amplification conditions were the same as those for *tax*. The probes were labeled with fluorescent 6-carboxyfluorescein (reporter) at the 5′ end and fluorescent 6-carboxytetramethylrhodamine (quencher) at the 3′ end. All samples were analyzed in duplicate. The DNA of freshly purified ATL cells, which harbor one copy of the HTLV-I provirus, was used as positive control, and its proviral load was given the value of 100% when used as point of comparison.

IL-PCR. In order to study the clonality of HTLV-I infected cells in hu-PBMC-NOG mice, we performed an inverse long PCR (IL-PCR) (10). Briefly, 1 μg of genomic DNA was first digested with EcoRI (TOYOBO, Osaka, Japan) and then self-ligated with T4 DNA ligase (TOYOBO) overnight at 4°C. Circularized DNA was then linearized with MluI (TOYOBO) to prevent amplification of the proviral sequence itself. The resulting DNA was used as template for IL-PCR, performed with LA *Taq* HS (Takara Bio Inc., Otsu, Japan). Amplification conditions were as follows: 94°C for 2 min; 40 cycles of 94°C for 30 s and 64°C for 10 min; and a final extension at 72°C for 15 min, using a Robocycler thermal cycler (Stratagene, La Jolla, CA). PCR products were electrophoresed in a 1% agarose gel and were then visualized via ethidium bromide staining.

Flow cytometric analysis. T-cell subsets of splenocytes were analyzed by flow cytometry (EPICS Coulter-Beckman, Fullerton, CA). Briefly, 10^6 cells were double stained with anti-human CD4-PC5 (Immunotech, Marseille, France) or anti-human CD8-PC5 (Immunotech) and anti-human CD45RO-fluorescein isothiocyanate (FITC) (Immunotech) or anti-human CD25-R-phycoerythrin (Caltag Laboratories, Burlingame, CA). They were also stained with anti-human CD45-FITC (Immunotech) and anti-mouse CD45-phycoerythrin (Immunotech) to assess the predominance of human cells in the recovered splenocytes. Cells were also stained with anti-human CD3-FITC (Sigma) and anti-human CD19-FITC (BD Biosciences, San Jose, CA).

Purification using magnetic beads. CD4$^+$ and CD8$^+$ T cells were isolated from 10^7 whole splenocytes by using BD IMag magnetic beads (BD Biosciences) according to the manufacturer's instructions. Positive selection of these T-cell subpopulations was performed using anti-human CD4- and anti-human CD8-conjugated magnetic particles.

Reverse transcriptase PCR (RT-PCR). RNA was extracted from splenic cells at the time of sacrifice and after 24 h of in vitro culture by using TRIzol reagent (Invitrogen, Carlsbad, CA) according to manufacturer's instructions. One microgram of total RNA was reverse transcribed by using the RNA LA PCR kit (using avian myeloblastosis virus) version 1.1 (Takara) using random primers. One microliter of cDNA was used as the PCR template. The following primers were used: 5′-CCGGCGCTGCTCTCATCCCGG-3′ and 5′-GGCCGAACATA GTCCCCCAGAG-3′ for *tax* and 5′-GCAGGGGGGAGCCAAAAGGG-3′ and 5′-TGCCAGCCCCAGCGTCAAAG-3′ for the GAPDH (glyceraldehyde-3-phosphate dehydrogenase) gene. The amplification conditions were as follows: 95°C for 2 min; 40 cycles of 95°C for 30 s, 62°C for 30 s, and 72°C for 30 s; and a final extension at 72°C for 2 min (for *tax*); 95°C for 3 min; 22 cycles of 95°C for 20 s, 57°C for 30 s, and 72°C for 1 min; and a final extension at 72°C for 7 min (for the GAPDH gene) in a thermal cycler (ASTEC, Fukuoka, Japan). PCR products were electrophoresed in a 2% agarose gel and visualized via ethidium bromide staining. For real-time PCR, an ABI PRISM 7500 sequence detector (Applied Biosystems) was used. Data were analyzed by a comparative cycle threshold method. The level of *tax* mRNA in the MT-1 cell line was used as a positive control and was assigned a value of 100 arbitrary units.

Sodium bisulfite treatment of genomic DNA. Sodium bisulfite treatment was performed as previously described (54). Briefly, 1 μg of genomic DNA was denatured in 0.3 N NaOH at 37°C for 15 min, and 1 μg of salmon sperm DNA was added to each sample to act as a carrier. Sodium bisulfite (pH 5.0) and hydroquinone were added to each sample to final concentrations of 3 M and 0.05 mM, respectively, and the reaction mixture was incubated at 55°C for 16 h. Samples were then desalted using the Wizard DNA cleanup system (Promega, Madison, WI). Finally, samples were desulfonated in 0.3 N NaOH at 37°C for 15 min.

COBRA. For a combined bisulfite restriction analysis (COBRA) (59), different regions of the HTLV-I provirus were amplified from sodium bisulfite-treated genomic DNA (54). The nested PCRs were performed using FastStart *Taq* DNA polymerase (Roche, Mannheim, Germany) under the following conditions: 95°C for 5 min; 40 cycles of 30 s at 95°C, 30 s at each annealing temperature, and 30 s at 72°C; and 2 min at 72°C for a final extension. The sequences of the primers used, and their annealing temperatures are as described previously (54). The PCR products were digested for at least 4 h with TaqI restriction enzyme, which resulted in a single recognition site within each product. The digested PCR products were separated in a 3% Nusieve 3:1 agarose (BMA, Rockland, ME) gel. The intensity of each fragment was determined by using a densitograph (version 4.0; ATTO, Tokyo, Japan).

Treatment with reverse transcriptase inhibitors in mice. hu-PBMC-NOG mice were inoculated with 10^3 MMC-treated MT-2 cells 3 days after transfer of human PBMC and were then divided into three groups for treatment with AZT (240 mg/kg of body weight/day) (Nacalai Tesque, Kyoto, Japan), tenofovir (130 mg/kg/day) (kindly provided by Gilead Sciences Inc., CA), or phosphate-buffered saline (PBS). They were treated immediately after MT-2 inoculation for 12 days and then sacrificed to recover spleens and cells from peritoneal lavage for analysis. Tenofovir and AZT were administered intraperitoneally 2 and 3 times a day, respectively. The control group was injected twice a day with PBS. In another experiment, two groups of mice received treatment with AZT for 7 days or tenofovir for 12 days beginning one week after infection with 10^3 or 10^5 MT-2 cells/mouse, respectively. Each independent experiment was performed using the PBMC from a single donor.

TABLE 1. Proviral load of mice inoculated with different numbers of MT-2 cells[a]

Donor	No. of MT-2 cells in inoculation	Proviral load (%)	
		Lavage specimen	Spleen
A	10^2	0.0	0.0
	10^3	0.3	0.0
	10^4	4.2	1.2
B	10^2	1.1	0.2
	10^3	2.5	0.4
	10^4	0.9	2.0
C	10^4	83.2	26.5
	10^5	97.9	71.7
	10^6	90.4	53.4

[a] Proviral loads of cells recovered from the peritoneal cavity and spleens 2 (for donors A and B) or 3 (for donor C) weeks after inoculation of the specified numbers of MT-2 cells are shown for mice initially receiving PBMC of three different human donors.

MTT assay. The inhibitory effects of tenofovir and AZT on cell growth were assessed by MTT [3-(4,5-dimethylthiazol-2-yl)-2,5-diphenyl tetrazolium bromide] assay, which is based on the reduction of MTT by metabolically active cells to a blue formazan that can be measured spectrophotometrically. PBMC of three different donors (10^5 cells/well) were cultured in the presence or absence of the RT inhibitors (serial 10-fold dilutions from 5 mM to 0.05 μM) and 20 U/ml of interleukin 2 (kindly provided by Shionogi & Co., Ltd., Osaka, Japan) in a 96-well plate for three days. Twenty microliters of MTT solution (7.5 mg/ml) was added to each well, and the plate was incubated at 37°C for 5 h. One hundred twenty microliters of the medium was removed and 100 μl of acidified isopropanol containing 4% (vol/vol) of Triton X was added to each well to dissolve the formazan crystals. Viability relative to the untreated control was determined. Drug concentrations which inhibited cell growth by 50% (i.e., 50% cytotoxic concentrations) were also calculated from these data. All assays were performed in quadruplicate.

RESULTS

De novo HTLV-1 infection of human PBMC in NOG mice. In order to establish an in vivo model for primary HTLV-1 infection of human lymphocytes, we chose NOG mice as recipients because they were proven to engraft human cells with high efficiency (25, 60). We first determined the number of MT-2 cells necessary to achieve infection in this new mouse model. We inoculated human PBMC of two different donors intraperitoneally and, three days later, injected different numbers of MMC-treated MT-2 cells, since HTLV-1 transmits efficiently only in a cell-to-cell fashion (23, 45, 61). Two weeks later, cells were recovered from the peritoneal cavity and the spleen of each mouse and proviral load was determined by real-time PCR (Table 1). A total of 10^3 MT-2 cells was enough to produce a detectable level of proviral load in both groups of NOG mice. Taking these results into account, we decided to use 10^3 or 10^4 MT-2 cells in the following experiments. Another group of mice was inoculated with 10^6 MT-2 cells and sacrificed 3 weeks later, which led to significantly increased proviral loads (Table 1).

To check the effects of different donor sources on proviral load, we inoculated PBMC from six healthy donors into NOG mice and found that the proportions of subpopulations in T and B lymphocytes did not influence proviral loads at 2 weeks after inoculation of MT-2 cells, and the proviral loads, even in mice inoculated with cells from the same donor, were variable, especially in cells from lavages (Table 2). Regarding provirus loads in spleen cells, variations were not so remarkable. In the following experiments, we used PBMC from a single donor in each experiment.

TABLE 2. Phenotypes of donor PBMC and proviral loads of cells recovered from infected hu-PBMC-NOG mice[a]

Donor	Surface markers of donor PBMC (%)[b]				Proviral load (%)	
	CD3	CD4	CD8	CD19	Lavage specimen	Spleen
D	69.7	61.8	18.7	12.2	3.7	0.6
					34.0	1.4
					2.8	0.5
E	84.7	53.4	33.9	3.0	0.6	0.1
					12.6	1.0
					11.6	0.8
F	67.0	48.0	31.9	2.8	0.2	0.0
					2.7	0.2
					0.6	0.1
G	74.9	43.9	37.7	1.3	7.4	0.2
					2.8	0.6
H	80.0	62.8	18.0	1.2	2.4	0.2
					0.4	0.0
I	ND	ND	ND	ND	20.5	2.5
					0.1	0.3

[a] PBMC from the indicated donors were transferred into NOG mice, and these were sacrificed 2 weeks after inoculation of 10^4 MMC-treated MT-2 cells.

[b] The percentage of cells positive for the specified markers before transfer into mice is shown for each donor.

[c] The proviral loads of human cells recovered from peritoneal lavage and spleens of the different mice are shown as percentages, calculated as described in Materials and Methods. ND, not determined.

In order to characterize the primary infection with HTLV-1, we inoculated a group of mice with 10^4 MT-2 cells after the transfer of PBMC and analyzed them in two groups at 2 and 4 weeks postinfection (p.i.). To assess the proportions of human cells in the studied specimens, we stained recovered cells with anti-mouse-CD45 and anti-human-CD45 antibodies and analyzed them by flow cytometry. Human cells accounted for at least 85% of the recovered splenocytes two weeks after the transfer and reached more than 94% in the group analyzed at 4 weeks p.i. (data not shown). The total number of recovered human lymphocytes was much larger than the number initially inoculated. Two weeks after the transfer of 10^7 human PBMC, we were able to recover $(7.7 \pm 3.4) \times 10^7$ human cells from the spleen of MT-2-inoculated mice and $(8.1 \pm 2.7) \times 10^7$ human cells from the spleen of the control group. These results demonstrate both migration from the peritoneal cavity to the spleen and in vivo cell expansion. There was no significant difference between the numbers of recovered splenocytes from the MT-2-inoculated and the uninoculated control groups, indicating that the cell proliferation was probably due to xenogeneic stimulation. This suggests that, in the early stages, many cells are stimulated to proliferate in the NOG mouse environment regardless of HTLV-1 infection.

In order to confirm HTLV-1 infection, we amplified a frag-

TABLE 3. Proviral load of in vivo infected cells[a]

Mouse	Proviral load (%)	
	Lavage specimen	Spleen
2-wk group		
2W-1	3.7	0.6
2W-2	34.0	1.4
2W-3	2.8	0.5
4-wk group		
4W-1	33.6	14.1
4W-2	48.1	12.9

[a] The percentages of the proviral load, calculated by comparison with a control DNA as described in Materials and Methods are shown for cells recovered from abdominal lavage and cells isolated from spleens of MT-2-inoculated hu-PBMC-NOG mice.

TABLE 4. Proviral load in $CD4^+$ and $CD8^+$ T cells[a]

Mouse	Proviral load (%)	
	$CD4^+$	$CD8^+$
2-wk group		
2W-1	0.6	0.7
2W-2	4.5	1.1
2W-3	1.2	0.4
4-wk group		
4W-1	14.9	7.8
4W-2	19.9	13.6

[a] Human $CD4^+$ and $CD8^+$ T cells were purified from 10^7 splenocytes of mice sacrificed at 2 or 4 weeks p.i. with the use of magnetic beads. Proviral load was determined by real-time PCR as described in Materials and Methods.

ment of the HTLV-1 pX region by using PCR, and proviral DNA was detected in the cells recovered from the MT-2-inoculated groups of hu-PBMC-NOG mice (data not shown). These PCR products were not derived from contamination of cellular DNA of MT-2 cells, since a PCR specific for one of HTLV-1 integration sites in MT-2 did not detect the provirus (data not shown). Splenocytes tended to have a lower proviral load than cells recovered from the peritoneal cavity. However, the proviral load in the 4-week group was generally greater than that from the 2-week group, suggesting the continuous proliferation of infected cells and propagation of the virus in this mouse model (Table 3).

Significant increase in the memory $CD4^+$ T-cell population after HTLV-1 infection. Although HTLV-1 is known to infect many types of cells in vivo (31), the majority of HTLV-1-infected cells are $CD4^+$ memory T cells (46, 62). To determine the effect of HTLV-1 infection on subpopulations of lymphocytes, we studied the expression of surface molecules by flow cytometry. Two weeks after infection, there was a significant increase in the cell population expressing CD4 and CD45RO

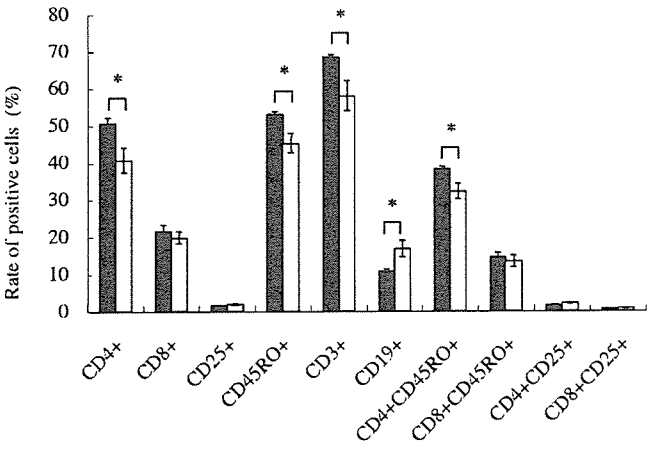

FIG. 1. Surface marker analysis of splenocytes in hu-PBMC-NOG mice. Splenocytes were isolated from hu-PBMC-NOG mice with or without HTLV-1 infection, and their surface markers were analyzed by flow cytometry. Splenocytes were recovered at 2 weeks p.i. The percentages of cells positive for various surface molecules are shown for MT-2-inoculated hu-PBMC-NOG mice (black bars) and uninfected controls (open bars). Values are means ± standard deviations from groups of three mice. * $P < 0.05$ (Student's t test).

molecules in the infected group compared to that in the control group (Fig. 1), suggesting that in the infected group of mice, memory $CD4^+$ T cells proliferated. This finding is consistent with observations with HTLV-1 carriers (62). The proviral loads in $CD4^+$ and $CD8^+$ splenic T cells were determined by real-time PCR (Table 4). As previously reported for HTLV-1 carriers, $CD8^+$ T cells were also found to contain the provirus, but to a lesser extent than $CD4^+$ T cells (39, 62). Nevertheless, proviral load tended to increase with time in both subpopulations of T cells (Table 4).

Polyclonal proliferation of HTLV-1-infected cells. In HTLV-1 carriers, polyclonal proliferation of HTLV-1 infected cells has been detected (10). Therefore, the clonality of HTLV-1-infected cells in hu-PBMC-NOG mice was analyzed by IL-PCR. We analyzed the same DNA samples in triplicate. When the same bands are detected in all three reactions, it means that the number of such clones is high. On the other hand, the stochastic results suggest that these clones are minor in vivo. As shown in Fig. 2, multiple bands were detected by IL-PCR at the 2-week time point, indicating an early polyclonal proliferation. At the 4-week time point, the number of bands increased, as did the intensity of bands corresponding to major clones, suggesting that both the numbers of clones and cell numbers of major clones increased (Fig. 2). We further confirmed the presence of different clones in the same mouse by determining the integration sites of the provirus in the human cells (data not shown).

Profile of proviral DNA methylation in primary HTLV-1 infection. Proviral DNA methylation appears to begin at the internal sequences, such as the *gag*, *pol*, and *env* regions (54), and accumulates in vivo. DNA methylation is thought to disturb viral gene transcription when the 5′ long terminal repeat (LTR) is methylated by inhibiting the binding of transcriptional factors (6). We analyzed the DNA methylation status of the proviral DNA in the cells recovered from the mice (Fig. 3). In the 2-week group, none of the three samples tested presented methylation in the *gag*, *pol*, or 5′ LTR regions. However, in the cells recovered from two mice after 4 weeks, the *gag* regions from both mice were partially methylated, and the *pol* region from one of the two mice was methylated. These results coincide with our previous findings that CpG motifs within the proviral sequence of HTLV-1 are methylated in a progressive manner, starting from internal regions and then spreading to the 5′ and 3′ ends of the provirus (54).

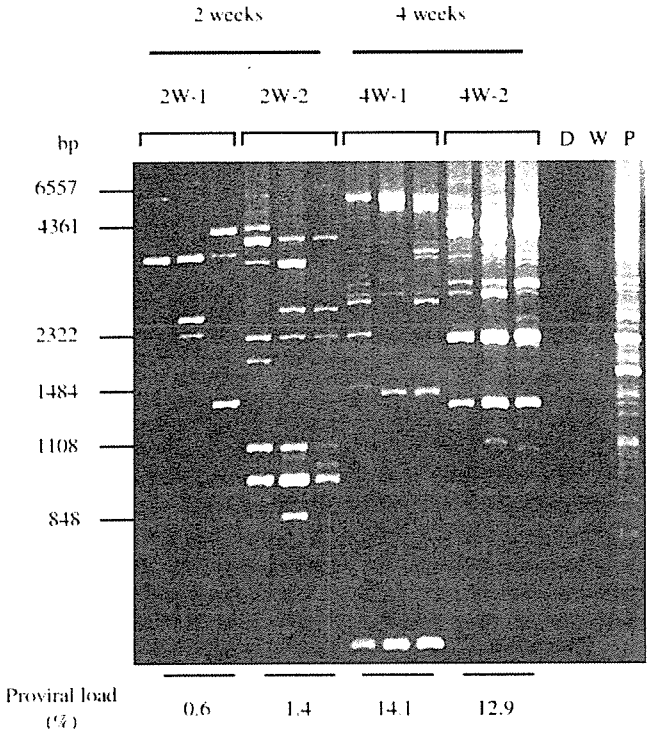

FIG. 2. Polyclonal proliferation of HTLV-I-infected cells in the spleens of hu-PBMC-NOG mice (2W-1, 2W-2, 4W-1, and 4W-2). Genomic DNA was isolated from recovered splenocytes and analyzed by IL-PCR as described in Materials and Methods. IL-PCR was performed in triplicate for each DNA sample. Genomic DNA was recovered from splenocytes at 2 or 4 weeks after injection of MT-2 cells. D, DNA of donor PBMC before inoculation; W, water; P, positive control (DNA from PBMC of an HTLV-I carrier). In addition, proviral load was quantified by real-time PCR as described in Materials and Methods and is shown as a relative percentage.

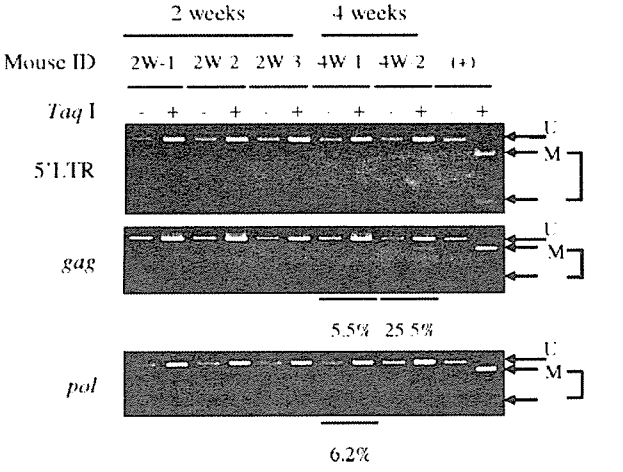

FIG. 3. DNA methylation of HTLV-I provirus. hu-PBMC-NOG mice were sacrificed 2 or 4 weeks after inoculation of MT-2 cells, and DNA methylation in the 5′ LTR, *gag*, and *pol* regions was studied by a COBRA assay. (+), positive control; U, intact fragment (unmethylated CpG); M, digested fragments (methylated CpG). Percentages of DNA methylation were calculated by densitography according to the following formula (with the variables as described above): [M/(U + M)] × 100.

Suppression of *tax* gene transcription in the NOG mouse model. The viral protein Tax is believed to play an important role in the proliferation of infected cells due to its pleiotropic functions (63). However, its expression in vivo has not been detected in most ATL patients (52). When ATL cells are transferred to culture ex vivo, Tax expression can be recovered (21, 30, 57). Viral gene transcription is also suppressed in PBMC of HAM/TSP patients, as well as asymptomatic HTLV-I carriers (19, 28). We performed an RT-PCR in order to detect *tax* mRNA in the spleens of infected hu-PBMC-NOG mice sacrificed 2 weeks p.i. (Fig. 4). Transcripts of the *tax* gene were undetectable in two of the three mice when cells were recovered, while the remaining one showed a low level of expression. In all three cases, there was an increase of *tax* gene transcription after 24 h of culture in vitro, even without changes in the proviral load (Fig. 4). Since this phenomenon occurs even in hu-PBMC-NOG mice, a factor(s) other than the host immune system must be involved in the suppression of *tax* gene transcription in vivo.

Effect of antiretroviral agents on HTLV-I infection. It is well known that HTLV-I is transmitted through sexual intercourse (49), breast feeding (48), and blood transfusions (42), and for transmission, cell-to-cell contact is thought to be essential. Due to the low capacity of cell-free virus to infect (8, 11), accidental exposures were not thought to confer a high risk of infection, and no prophylactic therapy has been considered. However, the prevalence of HTLV-I carriers among drug abusers shows that we do need to develop strategies to prevent viral transmission. A previous in vitro study reported that AZT was able to inhibit new HTLV-I infection of human lymphocytes (37). In addition, it has been reported that tenofovir efficiently inhibited the reverse transcriptase activity of HTLV-I (20). In order to assess whether a preventive antiretroviral treatment would prove useful in cases of accidental HTLV-I exposure, we treated hu-PBMC-NOG mice with two reverse transcriptase inhibitors, AZT and tenofovir. The treatment started as soon as MT-2 cells were injected and continued for 12 days. Proviral DNA was undetectable by real-time PCR in the groups of mice treated with AZT or tenofovir (Table 5). Mice seemed to tolerate the treatment without evident signs of toxicity. In the cases where weight loss was seen, it did not exceed 6% of the weight at the time treatment was started (data not shown). However, the number of human cells recovered from spleens of mice receiving AZT treatment was lower than those of the other two groups (Table 5), which indicates that this drug might be also interfering in the proliferation of transferred PBMC. In in vitro assays, we analyzed the cytotoxic effects of AZT and tenofovir on PHA-stimulated human PBMC derived from three different donors. We found that, in a range of concentrations from 5 mM to 0.05 μM, AZT was more toxic than tenofovir when used in incubations for 3 days (Fig. 5). The 50% cytotoxic concentration of AZT was 0.297 ± 0.169 mM, while that of tenofovir was higher than 5 mM. These results indicate that the cytotoxic effect of AZT contributes to suppression of the number of transferred human lymphocytes in our mouse in addition to inhibition of reverse transcriptase.

Clonal expansion of infected cells takes place even in the early stages of primary HTLV-I infection. It remains undeter-

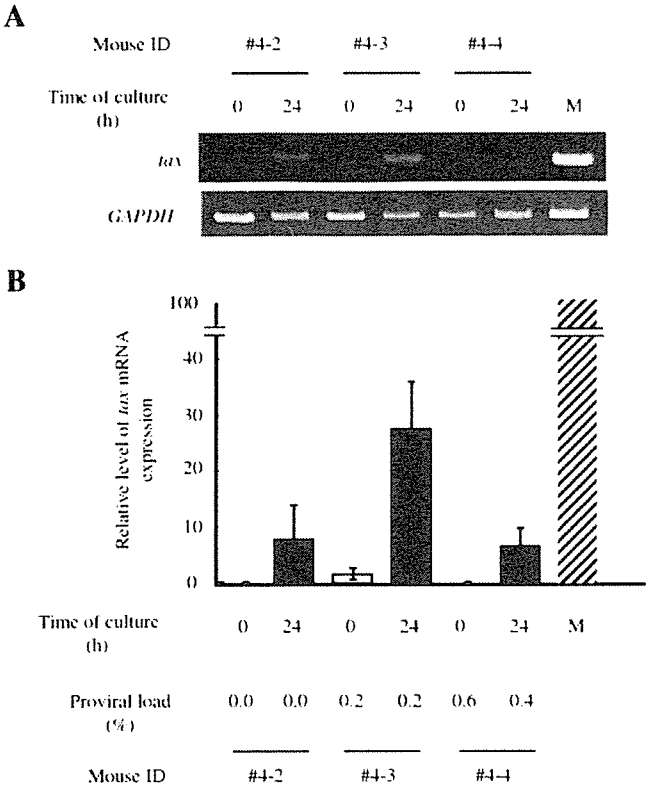

FIG. 4. Transcription of the *tax* gene increases after in vitro culture. Splenocytes of hu-PBMC-NOG mice inoculated with 10^4 MT-2 cells were recovered 2 weeks after infection. Transcription of the *tax* gene was quantified by semiquantitative PCR (A) or real-time PCR (B) at recovery and after 24 h of in vitro culture. Proviral loads for the same samples were also measured by real-time PCR. M, MT-1 cells; ID, identification number.

mined whether clonal proliferation or internal continuous contagion contributes to the increase of HTLV-1-infected cells. To answer this question, hu-PBMC-NOG mice infected with MT-2 cells were treated with tenofovir beginning 1 week after infection. Tenofovir treatment made no significant difference in HTLV-1 proviral load (Table 6), suggesting that clonal proliferation is predominant after HTLV-1 infection. The provirus loads of AZT-treated mice were lower than those of untreated mice, suggesting that the cytotoxic effect of AZT suppressed the provirus loads, as shown in Table 6.

DISCUSSION

Human immunodeficiency virus type 1 vigorously generates progeny virions through the action of its accessory genes, and the resulting free virions play an important role in its transmission, in addition to cell-to-cell transmission. In contrast, for HTLV-1, the efficiency of transmission by free virions is much lower than that via cell-to-cell contact (8), suggesting that HTLV-1 transmits primarily through the latter mechanism. To facilitate such transmission, instead of producing virions, HTLV-1 increases the number of infected cells by the actions of its accessory genes (17, 63). The finding that mother-to-infant transmission was more frequent in mothers with higher proviral loads indicates that such an increase in the number of

TABLE 5. RT inhibitors AZT and tenofovir inhibit de novo infection by HTLV-1[a]

Condition of treatment	Mouse	Proviral load (%)		Cell count (10^6)
		Lavage specimen	Spleen	
Untreated	C1	4.2	1.1	1.6
	C2	0.7	0.0	12.5
	C3	0.0	0.0	19.0
	C4	5.9	0.6	6.0
	C5	0.1	0.1	4.8
Tenofovir	T1	0.0	0.0	5.2
	T2	0.0	0.0	9.2
	T3	0.0	0.0	1.7
	T4	0.0	0.0	8.8
	T5	0.0	0.0	4.0
AZT	A1	0.0	0.0	2.6
	A2	0.0	0.0	3.6
	A3	0.0	0.0	4.5
	A4	0.0	0.0	2.2
	A5	0.0	0.0	2.3

[a] After human PBMC transfer and MT-2 inoculation (10^5 cells/mouse), mice were immediately subjected to antiretroviral therapy with AZT or tenofovir for 12 days. The control group was injected with PBS instead. Proviral loads were determined in cells recovered from the abdominal cavity and spleens. The total numbers of cells recovered from spleens are also shown.

infected cells facilitates the transmission of HTLV-1 (33). In vivo studies using animal models show that the early stage of HTLV-1 infection is controlled by accessory genes, including *p12*, *p13*, *p30*, and *HBZ* genes (3, 5, 22, 47). Thus, although in vivo studies using animal models revealed the importance of accessory genes in replication of HTLV-1 and proliferation of infected cells, the events in the early stages of in vivo transmission in human lymphocytes have not been studied yet due to the lack of an appropriate animal model. Since the metabolisms of nucleosides are quite different among animal species, it is critical to study the effect of reverse transcriptase inhibitors on HTLV-1 in human lymphocytes.

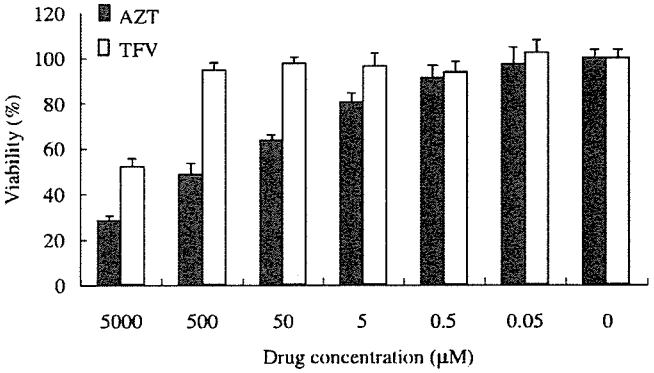

FIG. 5. Cytotoxic effects of tenofovir (TFV) and AZT in vitro. Human PBMC were stimulated with PHA for 3 days. Cells were then cultured in medium alone or medium containing the specified concentration of the indicated drug for another three days, at a density of 10^5 cells/well, in a 96-well plate. Viability was assessed by MTT assay as described in Materials and Methods. The results show the means ± standard deviations of quadruplicate measurements made in one of three representative experiments.

TABLE 6. Proviral load after treatment with tenofovir or AZT beginning one week after infection[a]

Condition of treatment	Mouse	Proviral load (%)	
		Lavage specimen	Spleen
Untreated	U11	7.4	1.7
	U12	0.1	0.0
	U13	15.4	1.9
	U14	3.8	0.7
Tenofovir	T11	0.0	0.0
	T12	0.2	0.0
	T13	15.9	1.8
	T14	14.5	2.6
Untreated	U21	0.6	0.1
	U22	ND	3.0
	U23	12.6	1.0
	U24	11.6	0.8
AZT	A21	0.0	0.0
	A22	ND	0.6
	A23	2.5	0.0
	A24	0.1	0.0

[a] After human PBMC transfer and MT-2 inoculation (10^3 cells/mouse for the tenofovir group, and 10^4 cells/mouse for the AZT group), mice were left for one week before starting treatment with tenofovir or AZT. The control groups were injected with PBS instead of the drugs. Mice were sacrificed 7 or 12 days after treatment with AZT or tenofovir, respectively. Splenocytes, as well as cells from the abdominal cavity, were recovered for analysis as described in Materials and Methods. ND, not determined.

It is widely accepted that the HTLV-1 virion per se is poorly infectious (8, 11) and that cell-to-cell transmission is more efficient both in vivo and in vitro (23, 42, 45, 61). Among drug abusers, HTLV-1 infection has been reported, indicating that HTLV-1 can be transmitted by the sharing of needles (12). Therefore, in cases of accidental exposure to HTLV-1-positive blood, preventive administration of antiretroviral drugs should be considered. In this study, we proved that the administration of a reverse transcriptase inhibitor beginning immediately after exposure can block HTLV-1 transmission. However, a delay in its administration may render it ineffective at preventing HTLV-1 transmission due to the importance of clonal expansion in the biology of this virus.

In particular, whether clonal expansion or internal continuous contagion is important in increasing the number of infected cells still remains unknown. A previous study reported that a reverse transcriptase inhibitor, lamivudine, reduced the proviral load in a patient with HAM/TSP (56), implicating internal contagion in maintaining the number of infected cells in vivo. However, another study reported that lamivudine had no definite effect on proviral load (34). In this study, administering tenofovir to block the spread of infection to new cells did not influence the proviral load in hu-PBMC-NOG mice, even though tenofovir has been reported to be more efficient in inhibiting HTLV-1 replication than lamivudine (20). Taken together, these results suggest that clonal proliferation contributes to the increase of HTLV-1-infected cells more than internal contagion even early in HTLV-1 infection. Recently, one study reported that clonality of HTLV-1-infected cells was variable after seroconversion but it became stable over time, indicating that the host immune system selected certain HTLV-1-infected clones (53). Since there is little or no host immune response to HTLV-1-infected cells in our system, it is possible that clonal proliferation of HTLV-1-infected cells is influenced by their ability to produce HTLV-1-encoded proteins, such as Tax. The factors including integration of the provirus in certain sites of the genome might also contribute to the variable proliferation of infected cells.

Viral gene transcription in HTLV-1-infected cells and ATL cells is suppressed in vivo. However, when they are cultured in vitro, transcription is rapidly recovered (54). Regarding the mechanisms of in vivo suppression, one possibility is that CTLs kill Tax-expressing cells, and the other is that nonimmune factors suppress it. The removal of $CD8^+$ T lymphocytes from PBMC derived from seropositive carriers enhanced Tax expression, suggesting that CTLs were indeed involved in inhibiting Tax expression in vivo (15, 18). On the other hand, a nonimmune factor(s) might be involved in this suppression. In this study, we showed that *tax* gene transcription was enhanced after in vitro culture. This finding is very similar to the phenomenon in carriers. It is noteworthy that in our system, there is no immune response to HTLV-1, indicating that a nonimmune factor(s) suppresses *tax* gene expression in vivo. These results suggest that both immune and nonimmune factors may be involved in the silencing of *tax* gene transcription.

Methylation of proviral DNA is regarded as a kind of host defense mechanism to suppress viral gene expression. However, HTLV-1 utilizes this epigenetic modification to escape the host immune surveillance. In cells immortalized by HTLV-1 in vitro, there was little DNA methylation in the provirus. In humans, on the other hand, DNA methylation accumulated within one year after seroconversion (54). In our system, DNA methylation was detected in the *pol* and *gag* regions 4 weeks after inoculation of MT-2 cells, indicating that HTLV-1 provirus is prone to methylation in vivo. Since *tax* gene transcription is silenced in hu-PBMC-NOG mice as shown in this study, such suppression might promote DNA methylation in vivo. On the other hand, since proliferation of HTLV-1-immortalized T lymphocytes is likely dependent on Tax expression, we speculate that cells with unmethylated provirus have growth advantages. We previously reported that histone H3 was hyperacetylated in the 5′ LTR of ATL cells without *tax* gene transcription, and such ATL cells transcribed *tax* gene within one hour after in vitro culture (54). This suggests the presence of a factor(s) inhibitory to *tax* gene transcription whose inhibition is nullified in in vitro culture. Such a mechanism, with the capacity for quickly switching on and off, would be useful for controlling *tax* gene transcription in vivo and thus enabling HTLV-1-infected cells to escape the host immune response.

In this study, we established an in vivo system for de novo infection with HTLV-1 and observed that the phenotype of HTLV-1-infected cells resembled that in the carrier state. The limitation of this in vivo system is that the long-term persistence of de novo infection in hu-PBMC-NOG mice cannot be examined, due to the graft-versus-host disease caused by implanted human lymphocytes. On the other hand, its merit is that the severe immune deficiency of this strain allows the vigorous proliferation of human lymphocytes, previously reported to be the result of a hyperactivation of the cells (40),

which enables HTLV-I to rapidly spread by cell-to-cell contact. Therefore, this model system should be a useful tool for analyzing the events in the early stage of HTLV-I infection in human lymphocytes.

ACKNOWLEDGMENTS

We thank Gilead Sciences Inc. for generously providing tenofovir for this study and Linda Kingsbury for excellent proofreading.

This study was supported by a grant-in-aid for scientific research from the Ministry of Education, Science, Sports, and Culture of Japan.

REFERENCES

1. **Akagi, T., I. Takeda, T. Oka, Y. Ohtsuki, S. Yano, and I. Miyoshi.** 1985. Experimental infection of rabbits with human T-cell leukemia virus type I. Jpn. J. Cancer Res. **76:**86–94.
2. **Albrecht, B., C. D. D'Souza, W. Ding, S. Tridandapani, K. M. Coggeshall, and M. D. Lairmore.** 2002. Activation of nuclear factor of activated T cells by human T-lymphotropic virus type 1 accessory protein p12^{I}. J. Virol. **76:**3493–3501.
3. **Arnold, J., B. Yamamoto, M. Li, A. J. Phipps, I. Younis, M. D. Lairmore, and P. L. Green.** 2006. Enhancement of infectivity and persistence in vivo by HBZ, a natural antisense coded protein of HTLV-1. Blood **107:**3976–3982.
4. **Bangham, C. R., and M. Osame.** 2005. Cellular immune response to HTLV-1. Oncogene **24:**6035–6046.
5. **Collins, N. D., G. C. Newbound, B. Albrecht, J. L. Beard, L. Ratner, and M. D. Lairmore.** 1998. Selective ablation of human T-cell lymphotropic virus type 1 p12I reduces viral infectivity in vivo. Blood **91:**4701–4707.
6. **Datta, S., N. H. Kothari, and H. Fan.** 2000. In vivo genomic footprinting of the human T-cell leukemia virus type 1 (HTLV-1) long terminal repeat enhancer sequences in HTLV-1-infected human T-cell lines with different levels of Tax 1 activity. J. Virol. **74:**8277–8285.
7. **Debacq, C., J. M. Heraud, B. Asquith, C. Bangham, F. Merien, V. Moules, F. Mortreux, E. Wattel, A. Burny, R. Kettmann, M. Kazanji, and L. Willems.** 2005. Reduced cell turnover in lymphocytic monkeys infected by human T-lymphotropic virus type 1. Oncogene **24:**7514–7523.
8. **Derse, D., S. A. Hill, P. A. Lloyd, H. Chung, and B. A. Morse.** 2001. Examining human T-lymphotropic virus type 1 infection and replication by cell-free infection with recombinant virus vectors. J. Virol. **75:**8461–8468.
9. **Dewan, M. Z., K. Terashima, M. Taniishi, H. Hasegawa, M. Ito, Y. Tanaka, N. Mori, T. Sata, Y. Koyanagi, M. Maeda, Y. Kubuki, A. Okayama, M. Fujii, and N. Yamamoto.** 2003. Rapid tumor formation of human T-cell leukemia virus type 1-infected cell lines in novel NOD-SCID/γc^{null} mice: suppression by an inhibitor against NF-κB. J. Virol. **77:**5286–5294.
10. **Etoh, K., S. Tamiya, K. Yamaguchi, A. Okayama, H. Tsubouchi, T. Ideta, N. Mueller, K. Takatsuki, and M. Matsuoka.** 1997. Persistent clonal proliferation of human T-lymphotropic virus type I-infected cells in vivo. Cancer Res. **57:**4862–4867.
11. **Fan, N., J. Gavalchin, B. Paul, K. H. Wells, M. J. Lane, and B. J. Poiesz.** 1992. Infection of peripheral blood mononuclear cells and cell lines by cell-free human T-cell lymphoma leukemia virus type I. J. Clin. Microbiol. **30:**905–910.
12. **Feigal, E., E. Murphy, K. Vranizan, P. Bacchetti, R. Chaisson, J. E. Drummond, W. Blattner, M. McGrath, J. Greenspan, and A. Moss.** 1991. Human T cell lymphotropic virus types I and II in intravenous drug users in San Francisco: risk factors associated with seropositivity. J. Infect. Dis. **164:**36–42.
13. **Feuer, G., J. A. Zack, W. J. Harrington, Jr., R. Valderama, J. D. Rosenblatt, W. Wachsman, S. M. Baird, and I. S. Chen.** 1993. Establishment of human T-cell leukemia virus type I T-cell lymphomas in severe combined immunodeficient mice. Blood **82:**722–731.
14. **Franchini, G., R. Fukumoto, and J. R. Fullen.** 2003. T-cell control by human T-cell leukemia/lymphoma virus type 1. Int. J. Hematol. **78:**280–296.
15. **Furuta, R. A., K. Sugiura, S. Kawakita, T. Inada, S. Ikehara, T. Matsuda, and J. Fujisawa.** 2002. Mouse model for the equilibration interaction between the host immune system and human T-cell leukemia virus type 1 gene expression. J. Virol. **76:**2703–2713.
16. **Gessain, A., F. Barin, J. C. Vernant, O. Gout, L. Maurs, A. Calender, and G. de The.** 1985. Antibodies to human T-lymphotropic virus type-I in patients with tropical spastic paraparesis. Lancet **ii:**407–410.
17. **Grassmann, R., M. Aboud, and K. T. Jeang.** 2005. Molecular mechanisms of cellular transformation by HTLV-1 Tax. Oncogene **24:**5976–5985.
18. **Hanon, E., S. Hall, G. P. Taylor, M. Saito, R. Davis, Y. Tanaka, K. Usuku, M. Osame, J. N. Weber, and C. R. Bangham.** 2000. Abundant tax protein expression in CD4+ T cells infected with human T-cell lymphotropic virus type I (HTLV-I) is prevented by cytotoxic T lymphocytes. Blood **95:**1386–1392.
19. **Hanon, E., J. C. Stinchcombe, M. Saito, B. E. Asquith, G. P. Taylor, Y. Tanaka, J. N. Weber, G. M. Griffiths, and C. R. Bangham.** 2000. Fratricide among CD8(+) T lymphocytes naturally infected with human T cell lymphotropic virus type I. Immunity **13:**657–664.
20. **Hill, S. A., P. A. Lloyd, S. McDonald, J. Wykoff, and D. Derse.** 2003. Susceptibility of human T cell leukemia virus type I to nucleoside reverse transcriptase inhibitors. J. Infect. Dis. **188:**424–427.
21. **Hinuma, Y., Y. Gotoh, K. Sugamura, K. Nagata, T. Goto, M. Nakai, N. Kamada, T. Matsumoto, and K. Kinoshita.** 1982. A retrovirus associated with human adult T-cell leukemia: in vitro activation. Gann **73:**341–344.
22. **Hiraragi, H., S. J. Kim, A. J. Phipps, M. Silic-Benussi, V. Ciminale, L. Ratner, P. L. Green, and M. D. Lairmore.** 2006. Human T-lymphotropic virus type 1 mitochondrion-localizing protein p13^{II} is required for viral infectivity in vivo. J. Virol. **80:**3469–3476.
23. **Igakura, T., J. C. Stinchcombe, P. K. Goon, G. P. Taylor, J. N. Weber, G. M. Griffiths, Y. Tanaka, M. Osame, and C. R. Bangham.** 2003. Spread of HTLV-I between lymphocytes by virus-induced polarization of the cytoskeleton. Science **299:**1713–1716.
24. **Imada, K., A. Takaori-Kondo, T. Akagi, K. Shimotohno, K. Sugamura, T. Hattori, H. Yamabe, M. Okuma, and T. Uchiyama.** 1995. Tumorigenicity of human T-cell leukemia virus type I-infected cell lines in severe combined immunodeficient mice and characterization of the cells proliferating in vivo. Blood **86:**2350–2357.
25. **Ito, M., H. Hiramatsu, K. Kobayashi, K. Suzue, M. Kawahata, K. Hioki, Y. Ueyama, Y. Koyanagi, K. Sugamura, K. Tsuji, T. Heike, and T. Nakahata.** 2002. NOD/SCID/gamma(c)(null) mouse: an excellent recipient mouse model for engraftment of human cells. Blood **100:**3175–3182.
26. **Johnson, J. M., C. Nicot, J. Fullen, V. Ciminale, L. Casareto, J. C. Mulloy, S. Jacobson, and G. Franchini.** 2001. Free major histocompatibility complex class I heavy chain is preferentially targeted for degradation by human T-cell leukemia lymphotropic virus type 1 p12^{I} protein. J. Virol. **75:**6086–6094.
27. **Kannagi, M., S. Harada, I. Maruyama, H. Inoko, H. Igarashi, G. Kuwashima, S. Sato, M. Morita, M. Kidokoro, M. Sugimoto, et al.** 1991. Predominant recognition of human T cell leukemia virus type I (HTLV-I) pX gene products by human CD8+ cytotoxic T cells directed against HTLV-I-infected cells. Int. Immunol. **3:**761–767.
28. **Kannagi, M., S. Matsushita, H. Shida, and S. Harada.** 1994. Cytotoxic T cell response and expression of the target antigen in HTLV-I infection. Leukemia **8**(Suppl. 1)**:**S54–S59.
29. **Kim, S. J., A. M. Nair, S. Fernandez, L. Mathes, and M. D. Lairmore.** 2006. Enhancement of LFA-1-mediated T cell adhesion by human T lymphotropic virus type 1 p12I1. J. Immunol. **176:**5463–5470.
30. **Kinoshita, T., M. Shimoyama, K. Tobinai, M. Ito, S. Ito, S. Ikeda, K. Tajima, K. Shimotohno, and T. Sugimura.** 1989. Detection of mRNA for the tax1/rex1 gene of human T-cell leukemia virus type I in fresh peripheral blood mononuclear cells of adult T-cell leukemia patients and viral carriers by using the polymerase chain reaction. Proc. Natl. Acad. Sci. USA **86:**5620–5624.
31. **Koyanagi, Y., Y. Itoyama, N. Nakamura, K. Takamatsu, J. Kira, I. Iwamasa, I. Goto, and N. Yamamoto.** 1993. In vivo infection of human T-cell leukemia virus type I in non-T cells. Virology **196:**25–33.
32. **Lairmore, M. D., L. Silverman, and L. Ratner.** 2005. Animal models for human T-lymphotropic virus type 1 (HTLV-1) infection and transformation. Oncogene **24:**6005–6015.
33. **Li, H. C., R. J. Biggar, W. J. Miley, E. M. Maloney, B. Cranston, B. Hanchard, and M. Hisada.** 2004. Provirus load in breast milk and risk of mother-to-child transmission of human T lymphotropic virus type I. J. Infect. Dis. **190:**1275–1278.
34. **Machuca, A., B. Rodes, and V. Soriano.** 2001. The effect of antiretroviral therapy on HTLV infection. Virus Res. **78:**93–100.
35. **Manel, N., F. J. Kim, S. Kinet, N. Taylor, M. Sitbon, and J. L. Battini.** 2003. The ubiquitous glucose transporter GLUT-1 is a receptor for HTLV. Cell **115:**449–459.
36. **Matsuoka, M., and K. T. Jeang.** 2005. Human T-cell leukemia virus type I at age 25: a progress report. Cancer Res. **65:**4467–4470.
37. **Matsushita, S., H. Mitsuya, M. S. Reitz, and S. Broder.** 1987. Pharmacological inhibition of in vitro infectivity of human T lymphotropic virus type I. J. Clin. Investig. **80:**394–400.
38. **Michael, B., A. M. Nair, H. Hiraragi, L. Shen, G. Feuer, K. Boris-Lawrie, and M. D. Lairmore.** 2004. Human T lymphotropic virus type-I p30II alters cellular gene expression to selectively enhance signaling pathways that activate T lymphocytes. Retrovirology **1:**39.
39. **Nagai, M., M. B. Brennan, J. A. Sakai, C. A. Mora, and S. Jacobson.** 2001. CD8(+) T cells are an in vivo reservoir for human T-cell lymphotropic virus type I. Blood **98:**1858–1861.
40. **Nakata, H., K. Maeda, T. Miyakawa, S. Shibayama, M. Matsuo, Y. Takaoka, M. Ito, Y. Koyanagi, and H. Mitsuya.** 2005. Potent anti-R5 human immunodeficiency virus type 1 effects of a CCR5 antagonist, AK602/ONO4128/GW873140, in a novel human peripheral blood mononuclear cell nonobese diabetic-SCID, interleukin-2 receptor gamma-chain-knocked-out AIDS mouse model. J. Virol. **79:**2087–2096.
41. **Nicot, C., M. Dundr, J. M. Johnson, J. R. Fullen, N. Alonzo, R. Fukumoto, G. L. Princler, D. Derse, T. Misteli, and G. Franchini.** 2004. HTLV-I-

encoded p30II is a post-transcriptional negative regulator of viral replication. Nat. Med. **10:**197–201.

42. **Okochi, K., and H. Sato.** 1984. Transmission of ATLV (HTLV-I) through blood transfusion. Princess Takamatsu Symp. **15:**129–135.
43. **Osame, M., K. Usuku, S. Izumo, N. Ijichi, H. Amitani, A. Igata, M. Matsumoto, and M. Tara.** 1986. HTLV-I associated myelopathy, a new clinical entity. Lancet **i:**1031–1032.
44. **Poiesz, B. J., F. W. Ruscetti, A. F. Gazdar, P. A. Bunn, J. D. Minna, and R. C. Gallo.** 1980. Detection and isolation of type C retrovirus particles from fresh and cultured lymphocytes of a patient with cutaneous T-cell lymphoma. Proc. Natl. Acad. Sci. USA **77:**7415–7419.
45. **Popovic, M., P. S. Sarin, M. Robert-Gurroff, V. S. Kalyanaraman, D. Mann, J. Minowada, and R. C. Gallo.** 1983. Isolation and transmission of human retrovirus (human T-cell leukemia virus). Science **219:**856–859.
46. **Richardson, J. H., A. J. Edwards, J. K. Cruickshank, P. Rudge, and A. G. Dalgleish.** 1990. In vivo cellular tropism of human T-cell leukemia virus type 1. J. Virol. **64:**5682–5687.
47. **Silverman, L. R., A. J. Phipps, A. Montgomery, L. Ratner, and M. D. Lairmore.** 2004. Human T-cell lymphotropic virus type 1 open reading frame II-encoded $p30^{II}$ is required for in vivo replication: evidence of in vivo reversion. J. Virol. **78:**3837–3845.
48. **Sugiyama, H., H. Doi, K. Yamaguchi, Y. Tsuji, T. Miyamoto, and S. Hino.** 1986. Significance of postnatal mother-to-child transmission of human T-lymphotropic virus type-I on the development of adult T-cell leukemia/lymphoma. J. Med. Virol. **20:**253–260.
49. **Tajima, K., S. Tominaga, and T. Suchi.** 1986. Malignant lymphomas in Japan: epidemiological analysis on adult T-cell leukemia/lymphoma. Hematol. Oncol. **4:**31–44.
50. **Takatsuki, K.** 2005. Discovery of adult T-cell leukemia. Retrovirology **2:**16.
51. **Takatsuki, K., T. Uchiyama, K. Sagawa, and J. Yodoi.** 1977. Adult T cell leukemia in Japan, p. 73–77. *In* S. Seno, F. Takaku, and S. Irino (ed.), Topic in hematology. The 16th International Congress of Hematology. Excerpta Medica, Amsterdam, The Netherlands.
52. **Takeda, S., M. Maeda, S. Morikawa, Y. Taniguchi, J. Yasunaga, K. Nosaka, Y. Tanaka, and M. Matsuoka.** 2004. Genetic and epigenetic inactivation of tax gene in adult T-cell leukemia cells. Int. J. Cancer **109:**559–567.
53. **Tanaka, G., A. Okayama, T. Watanabe, S. Aizawa, S. Stuver, N. Mueller, C. C. Hsieh, and H. Tsubouchi.** 2005. The clonal expansion of human T lymphotropic virus type 1-infected T cells: a comparison between seroconverters and long-term carriers. J. Infect. Dis. **191:**1140–1147.
54. **Taniguchi, Y., K. Nosaka, J. Yasunaga, M. Maeda, N. Mueller, A. Okayama, and M. Matsuoka.** 2005. Silencing of human T-cell leukemia virus type I gene transcription by epigenetic mechanisms. Retrovirology **2:**64.
55. **Tateno, M., N. Kondo, T. Itoh, T. Chubachi, I. Togashi, and T. Yoshiki.** 1984. Rat lymphoid cell lines with human T cell leukemia virus production. I. Biological and serological characterization. J. Exp. Med. **159:**1105–1116.
56. **Taylor, G. P., S. E. Hall, S. Navarrete, C. A. Michie, R. Davis, A. D. Witkover, M. Rossor, M. A. Nowak, P. Rudge, E. Matutes, C. R. Bangham, and J. N. Weber.** 1999. Effect of lamivudine on human T-cell leukemia virus type 1 (HTLV-1) DNA copy number, T-cell phenotype, and anti-Tax cytotoxic T-cell frequency in patients with HTLV-1-associated myelopathy. J. Virol. **73:**10289–10295.
57. **Uchiyama, T.** 1997. Human T cell leukemia virus type I (HTLV-I) and human diseases. Annu. Rev. Immunol. **15:**15–37.
58. **Uchiyama, T., J. Yodoi, K. Sagawa, K. Takatsuki, and H. Uchino.** 1977. Adult T-cell leukemia: clinical and hematologic features of 16 cases. Blood **50:**481–492.
59. **Xiong, Z., and P. W. Laird.** 1997. COBRA: a sensitive and quantitative DNA methylation assay. Nucleic Acids Res. **25:**2532–2534.
60. **Yahata, T., K. Ando, Y. Nakamura, Y. Ueyama, K. Shimamura, N. Tamaoki, S. Kato, and T. Hotta.** 2002. Functional human T lymphocyte development from cord blood CD34$^+$ cells in nonobese diabetic/Shi-scid, IL-2 receptor gamma null mice. J. Immunol. **169:**204–209.
61. **Yamamoto, N., M. Okada, Y. Koyanagi, M. Kannagi, and Y. Hinuma.** 1982. Transformation of human leukocytes by cocultivation with an adult T cell leukemia virus producer cell line. Science **217:**737–739.
62. **Yasunaga, J., T. Sakai, K. Nosaka, K. Etoh, S. Tamiya, S. Koga, S. Mita, M. Uchino, H. Mitsuya, and M. Matsuoka.** 2001. Impaired production of naive T lymphocytes in human T-cell leukemia virus type I-infected individuals: its implications in the immunodeficient state. Blood **97:**3177–3183.
63. **Yoshida, M.** 2001. Multiple viral strategies of HTLV-1 for dysregulation of cell growth control. Annu. Rev. Immunol. **19:**475–496.
64. **Zhang, W., J. W. Nisbet, B. Albrecht, W. Ding, F. Kashanchi, J. T. Bartoe, and M. D. Lairmore.** 2001. Human T-lymphotropic virus type 1 $p30^{II}$ regulates gene transcription by binding CREB binding protein/p300. J. Virol. **75:**9885–9895.
65. **Zhao, T. M., B. Hague, D. L. Caudell, R. M. Simpson, and T. J. Kindt.** 2005. Quantification of HTLV-I proviral load in experimentally infected rabbits. Retrovirology **2:**34.

HIV Encephalopathy

JMAJ 49(5・6): 212–218, 2006

Yoshiharu Miura,*1 Yoshio Koyanagi*1

Abstract

HIV encephalopathy is one of the most complex viral diseases. HIV-infection is mainly restricted to macrophages and microglia in HIV-infected brains, although HIV-induced damage extends to neurons and oligodendrocytes. Accumulating evidences suggest that HIV-encoded factors and other host factors are involved in the development of this disease: however, the precise mechanism remains unclear. In order to investigate this mechanism, we developed an HIV-1-infected human cell-transplanted mouse model (hu-PBMC-NOD-SCID mouse) and a coculture system with HIV-1-infected macrophages and murine or rat brain cells. Using these models, we have successfully determined that certain host factors are involved in the neuronal damage. Additionally, we are developing a screening system to identify the host factors that provide protection against HIV-1-induced encephalopathy. Our study will contibute to the development of a new therapeutic strategy for HIV encephalopathy and other CNS diseases.

Key words HIV encephalopathy, Macrophage, hu-PBMC-NOD-SCID mouse, A lentiviral screening system, Host factors, CNS diseases

Introduction

The human immunodeficiency virus type 1 (HIV-1) causes acquired immunodeficiency syndrome (AIDS) by the destruction of the immune system.[1–3] However, the target tissues are not restricted to those of the immune system. This virus invades the central nervous system (CNS) and induces a neurological disease called HIV encephalopathy. Most cases of this disease are diagnosed several years after the primary infection, and by then, the number of $CD4^+$ cells in the peripheral blood is significantly lower. The clinical symptoms of this disease include cognitive, behavioral, and motor dysfunction: these symptoms are characteristically found in subcortical dementia and commonly develop over a period of few months. In the early stage, forgetfulness and reduced concentration are frequently encountered and these are typically followed by short-term memory loss, carelessness and mental slowing. Motor disturbance in the form of leg weakness is sometimes observed at this stage. These symptoms often occur along with behavioral symptoms such as personality changes. Ataxia, tremor, pyramidal sign, and paresis are also found. On disease progression, the patient shows behavioral changes such as social withdrawal, apathy, akinetic and mute state.

New Problems After the Introduction of HAART

In 2004, approximately 40 million people worldwide were estimated to be already infected with HIV. However, a very effective anti-viral therapy called highly active antiretroviral therapy (HAART) that comprises a combination of HIV reverse transcriptase and protease inhibitors has been available since around 1997. Following the availability of this therapy, the number of deaths

*1 Laboratory of Viral Pathogenesis, Research Center for AIDS, Institute for Virus Research, Kyoto University, Kyoto
Correspondence to: Yoshiharu Miura MD, PhD, Laboratory of Viral Pathogenesis, Research Center for AIDS, Institute for Virus Research, Kyoto University, 53 Shougoin-kawaramachi, Sakyou-ku, Kyoto-shi, Kyoto 606-8507, Japan. Tel: 81-75-751-4813, Fax: 81-75-751-4812, E-mail: ymiura@virus.kyoto-u.ac.jp

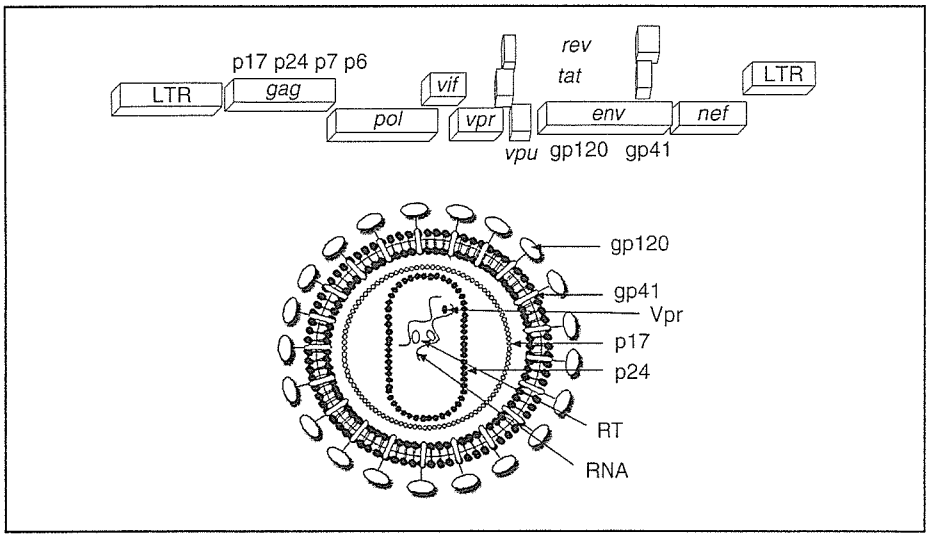

Fig. 1 The HIV-1 provirus and the virion structure

The genome consists with the LTRs (long terminal repeat), structural genes (*gag*, *pol*, and *env*), regulatory genes (*tat* and *rev*), and accessories genes (*nef*, *vif*, *vpr*, and *vpu*). The virion consists with Gag, Pol, Env, Vpr, and an RNA dimmer.

occurring due to AIDS has decreased, particularly in advanced countries. Although the incidence of HIV encephalopathy has markedly decreased due to this therapy,[4] in 2004, it was estimated that approximately 3 million patients worldwide continued to die of AIDS. Further, a less severe form of HIV encephalopathy that comprises a milder cognitive and motor disorder (MCMD) is now a potentially serious problem.[5] This syndrome is characterized by a much less pronounced state of memory loss and a decrease in computational and other higher cortical functions. The clinical presence of MCMD has been thought to be associated with the extent of pathological changes observed in the CNS due to HIV invasion. A potential explanation for the development of MCMD is that low level viral replication, as shown even in cases of highly HAART regimens, leads to the gradual progression of neurodegenerative damage.

The CNS of young children appears to be more vulnerable to the effect of HIV than that of adults. This is probably because in young children, the CNS is still in the developmental stage and contains many undifferentiated cells. The progression of pediatric AIDS is rapid and children do not respond to HAART. In addition, clinical analysis reveals that congenitally HIV-infected children frequently develop progressive encephalopathy, which is complicating microcephaly, spastic paraparesis, and delayed developmental milestones. After the introduction of HAART in many areas, the maternal-fetal transmission of HIV has been reduced successfully, thereby reducing the prevalence of progressive encephalopathy.

Currently, more than 6,500 people in Japan have been confirmed to be infected with HIV, and the number of HIV-infected persons is gradually increasing at a rate of 780 patients per year. Although the number of HIV encephalopathy patients clearly decreased after the introduction of the HAART, new problems such as the emergence of HAART-resistant viruses and the side effects of HAART are becoming apparent. Since subclinical MCMD patients appear to be increasing in many countries, HIV encephalopathy may also become a serious disease in Japan.

HIV and HIV Encephalopathy

HIV is virologically classified into HIV-1 and HIV-2. HIV-1 was initially isolated from a French patient in 1983, and subsequently, it has been identified as the causative agent of AIDS in many other countries. Currently, the HIV-1 epidemic has spread worldwide. It has been demonstrated that HIV-1 originated from chimpanzees:

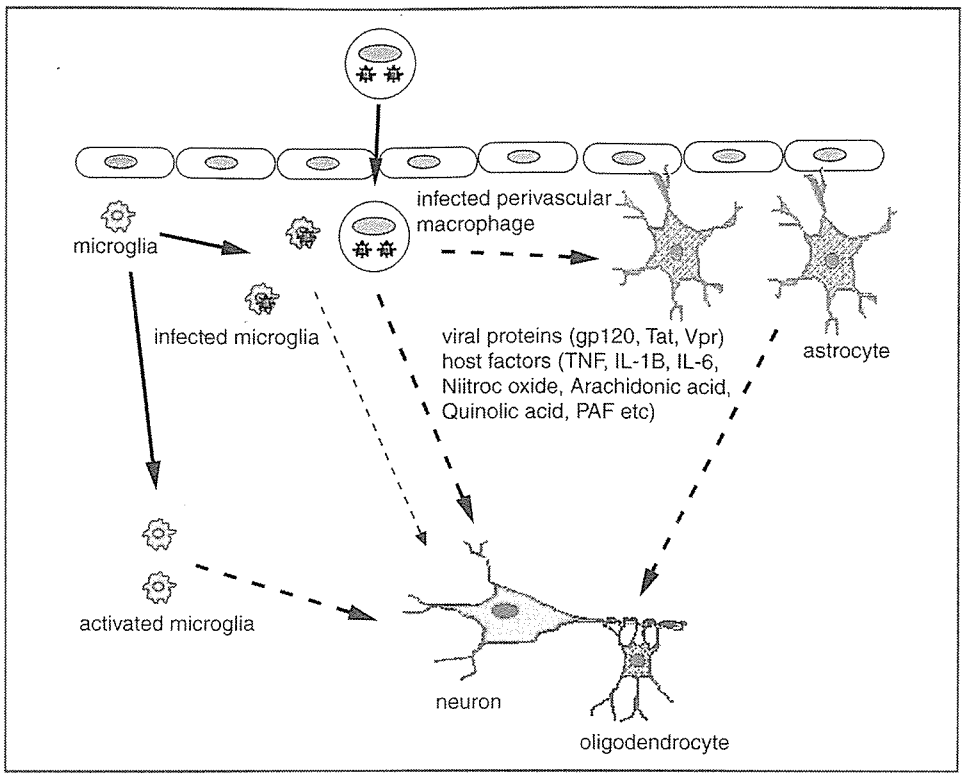

Fig. 2 Pathogenesis of HIV encephalopathy

Perivascular macrophages and microglia are responsible for producing HIV. They release viral proteins such as gp120, Tat, and Vpr and other host factors. Simultaneously, microglia and astrocytes are activated by these factors. Neuroprotective and neurodestructive factors coexist in this pathogenesis.

however, infected chimpanzees are resistant to the development of this disease. In 1986, HIV-2 was independently isolated from some patients in West Africa. Interestingly, in the case of HIV-2, it has been demonstrated that it originated in a small monkey species, such as the mangabee, and its potential for causing pathogenesis or acting as a pathogen in humans was clearly low. HIV-1 belongs to the retrovirus family, and its virion structure comprises 100-nm ball-like particles. Two viral RNAs, viral structural proteins, core protein p24, matrix protein p17, nucleocapsid p7, and the accessory protein Vpr are packed into its capsid, and the capsid is enveloped by two viral-encoded glycoproteins, namely, gp120 and gp41, and a plasma membrane-derived lipid (Fig. 1). When the HIV particles attach to the target human cells, gp120 on the viral surface specifically binds to the CD4 molecule on the plasma membrane of the target cells and subsequently to CXCR4 or CCR5, which are the physiological receptor molecules for different chemokines. In vivo, HIV replicates in the $CD4^+$ T cells and macrophages because both these cells express CD4 and CXCR4 or CCR5. Although these receptor positive cells get distributed in many lymphoid tissues such as the peripheral blood and lymph nodes, they rarely reside in the healthy brain. An examination of the autopsy samples of HIV encephalopathy patients revealed that HIV was predominantly found in the macrophages and microglia but not in the $CD4^+$ T cells located near the vessels. It is thought that the $CD4^+$ T cells are depleted in the peripheral blood at the time of development of HIV encephalopathy, and that they invade the brain very little. The typical pathological features of parenchymal infections include the activation of macrophages and astrocytes, cortical and central atrophy, diffuse myelin pallor, multinucleated giant cells, and microglial nodules. Furthermore, the macrophage-tropic virus, which uses CCR5

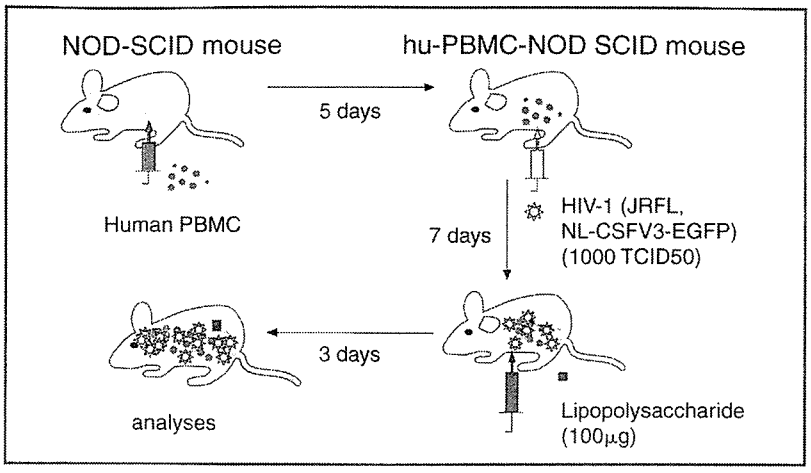

Fig. 3 A murine model using the hu-PBMC-NOD SCID mouse for HIV encephalopathy
Human peripheral blood monocytes were intraperitoneally transplanted into the immunodeficient NOD-SCID mouse. Macrophage-tropic HIV-1 and lipopolysaccharide were then intraperitoneally injected into the mouse.

as a coreceptor, is frequently isolated from the HIV-infected brain.[6] However, the T-tropic virus, which uses CXCR4, could not be detected. Interestingly, HIV does not replicate in neurons and oligodendrocytes, which are found to be severely damaged in the infected brains. Therefore, it has been postulated that macrophages and microglia are the key cell types that are affected in HIV, while the neurons and glia cells are damaged by the factors released from the infected macrophages and microglia in the infected brain. HIV-encoded proteins and host factors from the macrophage and glial cells may mutually influence the function and fates of neurons. Based on studies using an animal model, it is thought that HIV can enter the brain early after systemic infection. Although the CNS is physiologically separated by the blood-brain barrier (BBB), the mechanism of action of the BBB in HIV-infected brains and the critical factors that lead to the development of HIV encephalopathy remain unclear.

Several chemokines and their receptors have been the focus of the studies on the pathogenesis of HIV encephalopathy.[7] It has been reported that CXCL8 (IL-8), CXCL10 (IP10), CXCL12 (SDF-1α, β), CCL2 (MCP1), CCL3 (MIP1α), CCL4 (MIP1β), CCL5 (RANTES), CCL7 (MCP3), and CX3CL1 (Fractalkine) are involved in the development of HIV encephalopathy. CXCR1, CXCR2, CXCR3, CXCR4, CCR1, CCR2, CCR3, CCR5, and CX3CR1 are known to be expressed in the CNS and might have a various role in maintaining the balance between neuroprotection and neurodegeneration.

The infection of perivascular macrophages and microglia may cause a disruption in the normal neurological functions either by producing viral proteins, such as gp120,[8] Tat, and Vpr,[9] or by exerting an indirect or bystander effect via some neurotoxic factors.[10–12] In addition, it has been proposed that after the inflammatory process, due to the establishment of a self-sustaining chain reaction, viral infection might play a more limited role in the degenerative process. Although both these mechanisms are not mutually exclusive and might coexist, the bystander theory is probably more consistent with most of the evidence (Fig. 2).

Recently, a hypothesis that the CXCR4-using X4 virus emitted to the neurons has been suggested.[13] Although the X4 virus may act as a neurotoxic factor in vitro thus far, there is little evidence indicating that the X4 virus plays a critical role in the human CNS. HIV-1 has certain characteristics that differ from other simian-related viruses, namely, simian immunodeficiency virus (SIV) and simian human immunodeficiency virus (SHIV): the latter is a recombinant virus that is obtained by replacing the SIV envelope with an HIV envelope. The X4 virus frequently infects the neurons in SIV- and SHIV-infected models.

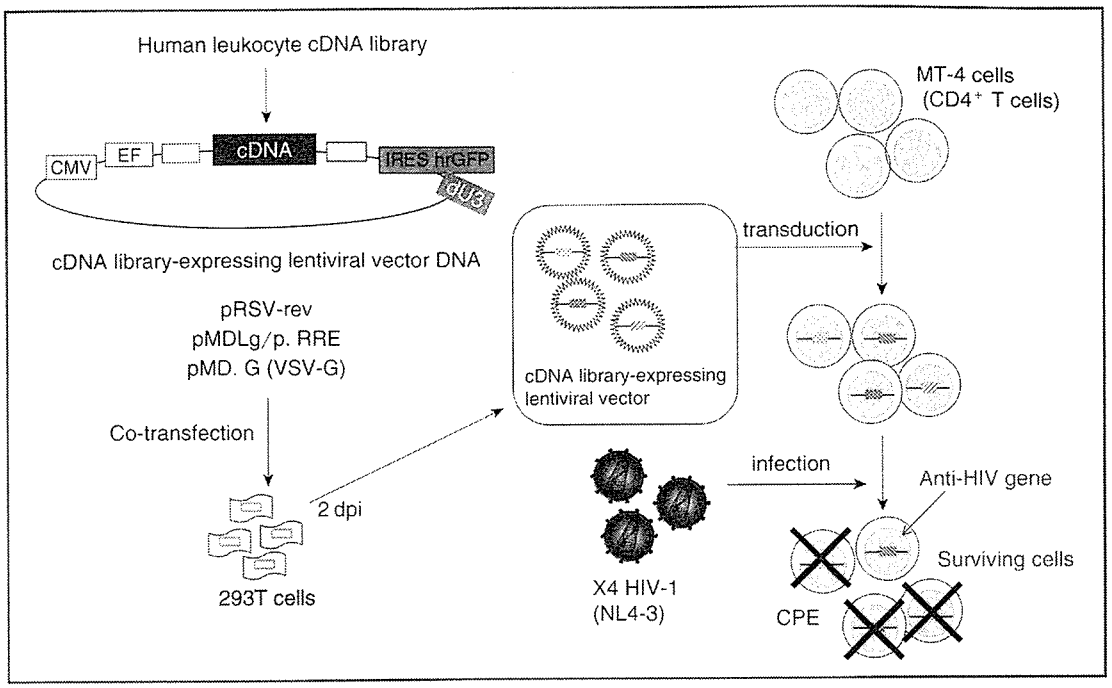

Fig. 4 The screening system used for the detection of the anti-HIV gene

A human leukocyte cDNA library was inserted into a vector and cotransfected with packaging plasmids into 293 T cells. The supernatant were transduced into MT-4 cells. They were infected with NL4-3 and the survivor cells were collected and analyzed.

By contrast, in the case of HIV-1, only the viruses using CCR5 have been found in the infected brain.

New Models of HIV Encephalopathy

We have developed an animal model of HIV encephalopathy. We used the NOD-SCID mouse, which represented severe immunodeficiency acquired through heredity, and produces human chimeric mice by the intraperitoneal transplantation of human peripheral blood mononuclear cells (PBMCs). HIV-1, which uses CCR5, was then inoculated intraperitoneally. After establishing systemic HIV-1 infection, a bacterial component lipopolysaccharide was injected intraperitoneally (Fig. 3). Infiltration of human T cells and macrophages was induced in the mouse brain and many of these cells were found to be infected with HIV-1. Further, the astrocytes and microglia were activated. Importantly, the apoptosis of neurons was frequently detected near the human macrophages infected with HIV-1. On the other hand, using the X4 virus, we observed that significant neuronal death was not detected in the brain. The TRAIL molecule, which is one of the death-inducing ligands, was found to be predominantly expressed in the HIV-1-infected macrophages in the brain. When a neutralizing antibody against human TRAIL was injected intraperitoneally, neuronal apoptosis was significantly inhibited. This suggests that the TRAIL molecule is important for guiding the apoptosis of neurons in HIV encephalopathy.[12] Therefore, we propose that the TRAIL molecule may play a role in HIV encephalopathy. Our proposal was further confirmed by the examination of human pathological autopsy samples and cultured human neurons.[14,15]

Based on these results, we are focusing on the analysis of HIV pathogenesis in the CNS using small animals such as mice and rats. These animals are very useful in neuroscientific studies because a considerable amount of scientific knowledges has been amassed using these animals. Several experiments using the cells of these small animals have been reported in HIV research.[16]

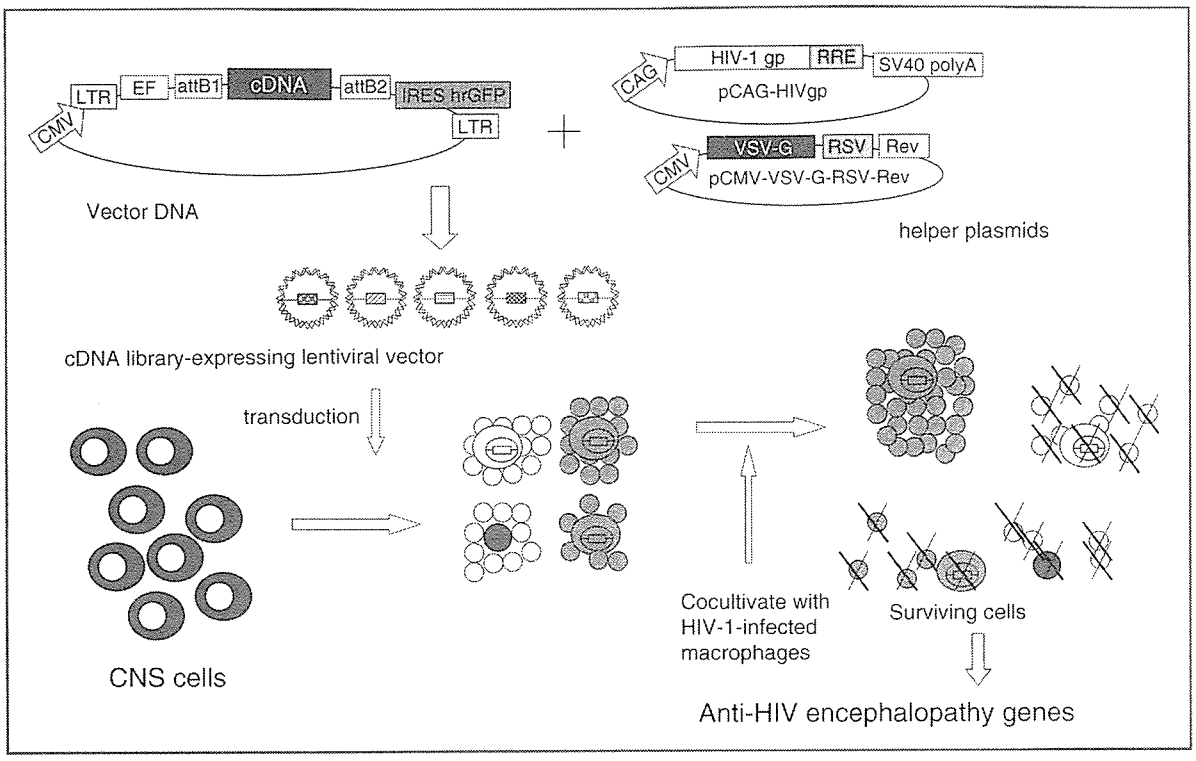

Fig. 5 The analyzing system of anti-HIV encephalopathy genes

The viral vectors expressing the rat brain cDNA were collected, transduced into the CNS cells, and cocultivated with HIV-1-infected macrophages. The surviving cells were then collected and analyzed.

Novel investigations have been carried out to determine the factors associated with this virus using a lentiviral vector system; this system was originally generated from HIV itself. We transduced the human leukocyte cDNA library into a human T cell line and then infected them with X4 HIV-1. After analyzing the gene that provides anti-HIV activity in the surviving cells, the CD14 gene[17] and an N-terminal deletion mutant of CD63 gene, namely CD63dN, were isolated (Fig. 4). CD14 appears to partially inhibit HIV-1 entry and provides resistance to HIV-1-induced cytopathic effect. CD63dN inhibits the surface expression of CXCR4. CD14 is one of the marker molecules of monocytes, and although the expression of CXCR4 can be seen in these cells, X4 virus cannot replicate efficiently in these cells. Further, since CD63 downregulates the activity of CXCR4 and the expression of CD63 is augmented in activated macrophages and microglia, it was suggested that CD63 might preferentially inhibit X4 HIV-1 infection in the infected brain. This explanation may be supported by the fact that it is difficult to detect X4 HIV-1 in the HIV-1-infected brain.

Further, we are trying to identify the genes that function against the cytopathic effect of HIV encephalopathy. An organic culture of the rat brains was cocultivated with the human macrophages with HIV infection. RNA was then collected from the samples of this culture, and was analyzed using a microarray system. Based on this analysis, the cDNA of a candidate gene was transduced into the rat brain cells and was cocultivated with HIV-infected human macrophages (Fig. 5). These experiments are currently in progress.

Conclusion

To date, the research on HIV encephalopathy has been carried out by analyzing the brain tissues of clinical specimens and by infecting experimental animals with SIV or SHIV. In addition to these

models, a novel approach has been initiated using small animals such as mice and rats. Based on previous reports, it is thought that many host factors as well as viral factors are closely involved in the pathogenesis of the HIV encephalopathy, and the elucidation of its mechanisms is very important. Further, new types of researches that aim at identifying additional host factors have been initiated by using a lentiviral vector. They can be applied to devise powerful new medical treatments. Finally, it is important to improve these systems using small experimental animals and lentivirus for various central nervous system diseases.

Acknowledgements

The authors wish to thank Professor Hidehiro Mizusawa (Department of Neurology and Neurological Science, Tokyo Medical and Dental University Graduate School of Medicine) for his collaboration, and Kitayama H, Andou Y, Aoki J, and Yoshida T (Institute for Virus Research, Kyoto University) for their assistance.

References

1. Miura Y, Koyanagi Y. Death ligand-mediated apoptosis in HIV infection. Rev Med Virol. 2005;15:169–178.
2. Badley AD, Roumier T, Lum JJ, Kroemer G. Mitochondrion-mediated apoptosis in HIV-1 infection. Trends Pharmacol Sci. 2003;24:298–305.
3. Arnoult D, Petit F, Lelievre JD, Estaquier J. Mitochondria in HIV-1-induced apoptosis. Biochem Biophys Res Commun. 2003; 304:561–574.
4. McArthur JC. HIV dementia: an evolving disease. J Neuroimmunol. 2004;157:3–10.
5. Brew BJ. Evidence for a change in AIDS dementia complex in the era of highly active antiretroviral therapy and the possibility of new forms of AIDS dementia complex. AIDS. 2004;18 (Suppl 1):S75–78.
6. Koyanagi Y, Miles S, Mitsuyasu RT, Merrill JE, Vinters HV, Chen IS. Dual infection of the central nervous system by AIDS viruses with distinct cellular tropisms. Science. 1987;236:819–822.
7. Martin-Garcia J, Kolson DL, Gonzalez-Scarano F. Chemokine receptors in the brain: their role in HIV infection and pathogenesis. AIDS. 2002;16:1709–1730.
8. Kaul M, Lipton SA. Chemokines and activated macrophages in HIV gp120-induced neuronal apoptosis. Proc Natl Acad Sci USA. 1999;96:8212–8216.
9. Patel CA, Mukhtar M, Pomerantz RJ. Human immunodeficiency virus type 1 Vpr induces apoptosis in human neuronal cells. J Virol. 2000;74:9717–9726.
10. Achim CL, Heyes MP, Wiley CA. Quantitation of human immunodeficiency virus, immune activation factors, and quinolinic acid in AIDS brains. J Clin Invest. 1993;91:2769–2775.
11. Adamson DC, McArthur JC, Dawson TM, Dawson VL. Rate and severity of HIV-associated dementia (HAD): correlations with Gp41 and iNOS. Mol Med. 1999;5:98–109.
12. Miura Y, Misawa N, Kawano Y, et al. Tumor necrosis factor-related apoptosis-inducing ligand induces neuronal death in a murine model of HIV central nervous system infection. Proc Natl Acad Sci USA. 2003;100:2777–2782.
13. Zheng J, Thylin MR, Ghorpade A, et al. Intracellular CXCR4 signaling, neuronal apoptosis and neuropathogenic mechanisms of HIV-1-associated dementia. J Neuroimmunol. 1999; 98:185–200.
14. Miura Y, Koyanagi Y, Mizusawa H. TNF-related apoptosis-inducing ligand (TRAIL) induces neuronal apoptosis in HIV-encephalopathy. J Med Dent Sci. 2003;50:17–25.
15. Ryan LA, Peng H, Erichsen DA, et al. TNF-related apoptosis-inducing ligand mediates human neuronal apoptosis: links to HIV-1-associated dementia. J Neuroimmunol. 2004;148:127–139.
16. Persidsky Y, Limoges J, McComb R, et al. Human immunodeficiency virus encephalitis in SCID mice. Am J Pathol. 1996;1 49: 1027–1053.
17. Kawano Y, Yoshida T, Hieda K, Aoki J, Miyoshi H, Koyanagi Y. A lentiviral cDNA library employing lambda recombination used to clone an inhibitor of human immunodeficiency virus type 1-induced cell death. J Virol. 2004;78:11352–11359.

ELSEVIER

Journal of Immunological Methods 311 (2006) 47–56

JIM
Journal of Immunological Methods

www.elsevier.com/locate/jim

Research paper

Novel two-parameter flow cytometry (MIL4/SSC followed by MIL4/CT7) allows for identification of five fractions of guinea pig leukocytes in peripheral blood and lymphoid organs

Mari Takizawa [a], Joe Chiba [b], Shinji Haga [c], Toshihiko Asano [d], Tsuyoshi Yamazaki [e], Naoki Yamamoto [a], Mitsuo Honda [a,*]

[a] *AIDS Research Center, National Institute of Infectious Diseases, Tokyo, 162-8640, Japan*
[b] *Department of Biological Science and Technology, Science University of Tokyo, Chiba, 278-0022, Japan*
[c] *Department of Bacteriology, National Institute of Infectious Diseases, Tokyo, 162-8640, Japan*
[d] *Division of Experimental Animal Research, National Institute of Infectious Diseases, 162-8640, Tokyo, Japan*
[e] *School of High Technology for Human Welfare, Tokai University, Shizuoka, 410-0395, Japan*

Received 22 June 2005; received in revised form 19 December 2005; accepted 4 January 2006
Available online 21 February 2006

Abstract

Though the guinea pig has been an extremely useful animal model for a variety of diseases, the tools necessary to undertake a full-scale immunological analysis of the guinea pig have been lacking. For instance, traditional two-parameter forward/side scatter (FSC/SSC) flow cytometry, though effective in human and other animal models, is unable to adequately identify the distinct fractions of guinea pig peripheral blood leukocytes (PBL). We introduce here a new flow cytometric technique (MIL4/SSC followed by MIL4/CT7) which redresses this lack by identifying and characterizing five distinct fractions of PBL: neutrophils, lymphocytes, monocytes, eosinophils plus basophils, and the novel MIL4$^-$SSC^{large}CT7^{high} population. The MIL4$^-$SSC^{large}CT7^{high} cells possess cytoplasmic inclusion bodies of variable size that were positive for periodic acid Schiff (PAS). Their cell surface stained positive for the helper/inducer lymphocyte markers, T cell markers, CD45, Thy-1, asialo GM1 and FcR, but negative for B cell markers, such as membrane-type IgM, CD8 and MHC class II. The novel flow cytometric technique also allowed us to establish that the five leukocyte fractions were found in PBL, splenocytes, thymocytes and lymph node cells. Cells which were positive for inclusion bodies comprised 16.6% of splenocytes, 9.9% of PBL and 4.3% of liver cells, but were comparatively rare in lymph node cells, thymocytes, and BM cells. The novel flow cytometric technique introduced here will allow a better understanding of the response of each type of guinea pig leukocyte and thereby shed light on the diseases with which they are associated.

Keywords: Guinea pig; Leukocyte fraction; Flow cytometry; Cell surface marker

Abbreviations: BCG, bacillus Calmette and Guérin; MHC, major histocompatibility complex; PBL, peripheral blood leukocytes; CTL, cytotoxic T lymphocyte; MIL4$^-$SSC^{large}CT7^{high}, MIL4$^-$side scatter^{large}CT7^{high}; NIID, National Institute of Infectious Diseases; FITC, fluorescein isothiocyanate; PE, phycoerythrin; mAb, monoclonal antibody; APC, allophycocyanin; LN, lymph node; BM, bone marrow; PI, propidium iodide; PAS, periodic acid Schiff; PMN, polymorphonuclear neutrophils.

* Corresponding author. Tel.: +81 3 5285 1111; fax: +81 3 5285 1183.
E-mail address: mhonda@nih.go.jp (M. Honda).

0022-1759/$ - see front matter © 2006 Elsevier B.V. All rights reserved.
doi:10.1016/j.jim.2006.01.010

1. Introduction

For more than 100 years, guinea pigs have been an important animal model for the study of *Mycobacterium tuberculosis* (*M. tuberculosis*), the vaccine strain *M. bovis* bacillus Calmette and Guérin (BCG) (Bloom and Fine, 1994) and other infectious agents (Griffith and Aquino-de Jesus, 1991; Myers and Connelly, 1992; Stanberry, 1995; Wicher and Wicher, 2001; Woolf, 1991); carcinoma (Van der Meijden et al., 1989); allergies (Broder et al., 1978; Daffonchio et al., 1989; Gulbenkian et al., 1990; Kallos and Kallos, 1984; Samejima et al., 1988; Tohda et al., 2001); and various other biological phenomena (Wagner and Manning, 1976).

Though an animal model of considerable importance, guinea pigs pose some immunological limitations not seen in other models. For instance, in humans PBL leukocyte fractions of granulocytic, lymphoid or mononuclear phagocytic origins are easily identified (Abramson et al., 1977; Prchal et al., 1978) using traditional flow cytometry, and terminally differentiated cells within those fractions are known to function cooperatively as a major defense against foreign pathogens (Ginaldi et al., 1999; Silva et al., 1989; Paul, 1993, 1999; Zhang et al., 1992). However, those fractions cannot be clearly identified in guinea pigs using standard two-parameter forward/side scatter (FSC/SSC) flow cytometric analysis (Choong et al., 1995; Goto and Nishioka, 1989; Lanza et al., 1992).

Other obstacles to the identification of distinct PBL populations in guinea pigs include the lack of phenotypic characterization of cell surface markers due to the limited availability of anti-guinea pig antibodies (only ten clones are available), the paucity of genetic data on guinea pig MHC haplotypes, the lack of well-established animal strains, and the lack of data on the functional properties of guinea pig leukocytes, for example cytotoxic T lymphocyte (CTL) activity. Finally, guinea pig spleen cells do not always respond well to immunogens, underscoring the challenge of using these animals in immunologic studies.

To help redress these problems, we found cross-reactivity of porcine m-Ab MIL4 (Haverson et al., 1994) and here introduce a new flow cytometric technique (MIL4/SSC followed by MIL4/CT7 antibodies) capable of clearly differentiating five distinct fractions of guinea pig leukocytes: neutrophils; monocytes; lymphocytes; eosinophils plus basophils; and the novel MIL4^{-}side scatter^{large}CT7^{high} (MIL4^{-}SSC^{large}CT7^{high}) leukocytes. We also used this technique to characterize the fractions and to normalize tissue distribution.

2. Materials and methods

2.1. Animals

Female Hartley guinea pigs, 4 to 6 weeks of age and weighing 350 to 400 g each, were obtained from Japan SLC, Inc., Shizuoka, Japan. Animals used in the studies were free of pathogenic bacteria and parasites. They were housed in accordance with the guidelines for animal experimentation of the Japanese Association for Laboratory Animal Science, 1987, in full compliance with the Law for the Humane Treatment and Management of Animals (in Japan). Animals were fed and maintained in accordance with the guidelines set forth by the Institutional Animal Care and Use Committee of National Institute of Infectious Diseases (NIID), Japan. Once approved by an institutional committee for animal experiments, these studies were conducted at the Animal Facility of Toyama Campus, NIID, Japan, in accordance with the requirements specifically stated in the Laboratory Biosafety Manual of the World Health Organization.

2.2. Antibodies

The anti-guinea pig antibodies used in this study are listed in Table 1. Fluorescein isothiocyanate (FITC)-

Table 1
Panel of anti-guinea pig mAbs used for flow cytometry[a]

Clone	Specificity	Ig class
Msgp9	Pan B-cell	IgG1
31D2	IgM	IgG
R27E	MHC Class II	IgG
20ED7	FcR	IgG
CT5	Pan T-cell	IgG1
H159	Pan T-cell	IgG
CT7	CD4 (T helper/inducer)	IgG1
H155	T helper/inducer	IgG
H154	Thy-1	IgG
CT6	CD8 (T suppressor/cytotoxic)	IgG1
MIL4	Porcine neutrophils and eosinophils	IgG1
Asialo GM1	Mouse and rat NK cells	Polyclonal rabbit Ig
IH-1	LCA (leukocyte common antigen)	IgG1
H201	LCA (leukocyte common antigen)	IgG

[a] Anti-guinea pig mAbs R27E, 31D2, 20ED7, H159, H155, H154 and H201 were the kind gift of Dr. R. Burger, Robert Koch Institute, Berlin, Germany. Asialo GM1 was obtained from Wako Pure Chemicals, Ltd., with the rest obtained from Serotec.

labeled T helper/inducer (CT7) cells, anti-CD8 cells (CT6, Samejima et al., 1988), anti-B cells (Msgp9) and anti-T cells (CT5, Broder et al., 1978), along with the purified anti-porcine neutrophil subset (MIL4, Haverson et al., 1994), anti-CD45 (IH-1) and phycoerythrin (PE)-labeled rabbit anti-mouse IgG-F(ab')$_2$ were obtained from Serotec, Ltd. (Oxford, UK). The MIL4 monoclonal antibody (mAb) was labeled with FITC and biotin by conventional methods. Streptavidin–allophycocyanin (APC) and streptavidin–cychrome was purchased from Pharmingen (San Diego, CA, USA). Antibodies to guinea pig MHC class II antigens (R27E7), IgM (31D2), leukocyte common antigen (LCA, H201), an additional T cell antigen (H159), an additional T helper/inducer antigen (H155), Thy-1 (H154) and Fc receptors (20ED7) were kindly supplied by Dr. R. Burger, Department of Immunology, Robert Koch-Institute, Nordufer 20, D-13353, Berlin, Germany (Burger et al., 1981; Schafer and Burger, 1991; Steerenberg et al., 1991). Anti-guinea pig Fc receptor (20ED7) was prepared by one of us (Chiba, unpublished). Anti-asialo GM1 was obtained from Wako Pure Chemicals, Ltd. (Tokyo, Japan). Anti-human CD56 antibodies used in the study were NCAM16.2 (Becton Dickinson, San Jose, CA, USA), MY 31 (Becton Dickinson), B159 (Pharmingen), NKI-nbi-1, (Nichirei Bioscience Inc., Tokyo, Japan) and NKH-1 (Beckman Coulter, Florida, USA).

2.3. Cells and isolation of leukocyte subsets

Splenocytes, lymph node (LN) cells, thymocytes and liver cells were teased out by pressing organ fragments through a mesh filter cell strainer (Becton Dickinson). PBL, liver cells, bone marrow (BM) cells and splenocytes were hemolysed using a lysis buffer consisting of 0.15 M NH_4Cl, 0.1 mM EDTA-2Na, 1.0 mM $KHCO_3$. After being washed twice, the cells were resuspended in PBS-staining buffer with 0.1% NaN_3 and 3% FCS.

2.4. Flow cytometric analysis of PBL and immune cells by their cell-surface staining with specific monoclonal antibodies

First, normal guinea pig γ-globulin was purified by 33% by subjecting it to two courses of ammonium sulfate precipitation and then incubated with cells at a final concentration of 1 mg/ml at 4 °C for 10 min to prevent nonspecific binding of the specific antibodies, except for asialo GM1 (Nakahara et al., 1980), FcR, and IgM staining. Then, we added a purified antibody and incubated for a further 30 min before washing and adding a PE-conjugated rabbit anti-mouse IgG F (ab) at 4 °C for 30 min. FITC-conjugated and biotin-conjugated antibodies were incubated with the cells at 4 °C for 30 min. Finally, we incubated the cells with streptavidin APC and streptavidin cychrome at 4 °C for 30 min and washed with staining buffer. Dead cells were excluded by propidium iodide (PI) and viable cells were analyzed on a FACScalibur (Becton-Dickinson, San Jose, CA, USA) equipped with an argon and semiconductor laser sets at 488 and 635 nm using Cell Quest software (Becton-Dickinson).

2.5. Morphological studies

Sorted cells were cytocentrifuged using a Cytospin-3 (Shandon Life Sciences International, Ltd., Runcorn, UK) and stained with May–Giemsa solution (Merck KGaA, Darmstadt, Germany) or periodic acid Schiff (PAS) (MUTO Pure Chemicals Co., Ltd., Tokyo, Japan), as described elsewhere.

2.6. Statistical analysis

Data analysis was carried out using the Stat View program (SAS Institute, Cary, NC) and data are expressed as the mean±SD.

3. Results

3.1. Evaluation of guinea pig leukocytes by conventional flow cytometry

As noted above, one of the drawbacks of studying immunologic responses in guinea pigs is the difficulty of identifying distinct PBL populations by conventional assay methods (guinea pig PBL, 1A-a; and human PBL, 1B-a). We found that one reason for the difficulty in gating guinea pig PBL was a unique population of cells in guinea pigs (the gated cell population in 1A-b), not present in humans (no corresponding cells in the gated area in Fig. 1B-b), that stains highly positive for the helper/inducer marker CT7 and SSC (the gated cell population in Fig. 1A-b). When the $SSC^{large}CT7^{high}$ population was deleted from guinea pig PBL in the cytometric analysis data, the three distinct populations of lymphocytes, gated with green circles; monocytes, gated with red circles; and granulocytes, gated with blue circles, could be clearly visualized using the conventional FSC/SSC flow cytometry of guinea pig PBL (Fig. 1A-c).

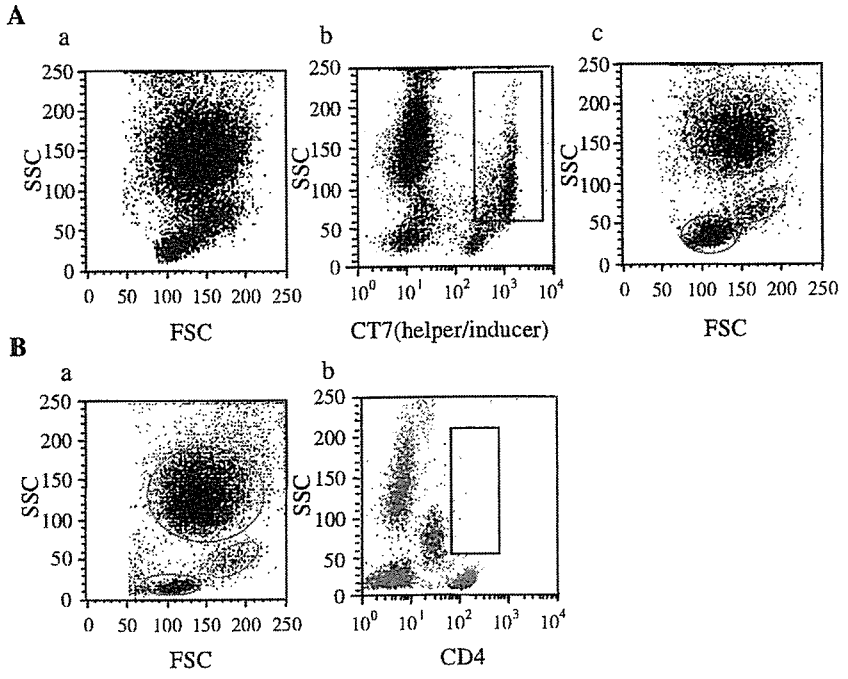

Fig. 1. Comparison of guinea pig and human PBL by two-parameter flow cytometric assays using light scatter and anti-CT7 (helper/inducer) mAb. Viable cells were gated by FSC/SSC after excluding dead cells using propidium iodide. A. Separation of guinea pig PBL fractions: (a) unsuccessful separation of guinea pig PBL by conventional FSC/SSC two-parameter flow cytometry. (b) Another separation of the PBL by CT7/SSC two-parameter flow cytometry. (c) Distribution of PBL after removal of the $SSC^{high}CT7^{high}$ population which was located in the gated population of Fig. 1A-b. B. Separation of human PBL fractions. Two-parameter flow cytometric separation of PBL by (a) FSC/SSC and (b) CD4/SSC. Each gated color population from humans was equivalent to the color indicated by SSC and CD4: lymphocytes (green), monocytes (red), and granulocytes (blue). Gate in Fig. 1B-b contained a SSC^{high}CD4-positive population.

3.2. The unique PBL fraction is further identified as $MIL4^{-}SSC^{large}CT7^{high}$

By screening human and mouse mAbs that cross-react with guinea pig cell surface antigens, we identified one antibody MIL4 that proved useful in differentiating guinea pig PBL into four subpopulations using two-parameter, consecutive MIL4/SSC flow cytometry (Fig. 2A). That antibody had previously been shown to recognize porcine neutrophils, eosinophils and basophils (Haverson et al., 1994). However, the CD antigen which was recognized by this antibody has not been defined (Haverson et al., 1994). By comparing the flow charts of guinea pig PBL obtained using a two-parameter MIL4/SSC analysis (Fig. 2A) with that obtained using a FSC/SSC analysis (Fig. 2B), we were able to identify four distinct PBL subpopulations: lymphocytes (green), monocytes (red), granulocytes (blue) and a novel $MIL4^{-}SSC^{large}$ population (orange). As shown in Fig. 2D, we further separated the $MIL4^{-}SSC^{large}$ subpopulation (orange) by gating with MIL4/CT7 into $MIL4^{-}CT7^{high}$ cells (approximately 84±6%) of the $MIL4^{-}SSC^{large}$ cells and $MIL4^{-}CT7^{-}$ cells (approximately 16±3%, gated population of Fig. 2D). Thus, we separated guinea pig PBL into 5 distinct subpopulations.

3.3. Morphological confirmation of the five leukocyte fractions isolated by cell sorting

We first sorted the green, red and blue leukocyte fractions in Fig. 2A with a FACS Vantage and morphologically confirmed them as guinea pig lymphocyte, monocyte and granulocyte fractions, respectively, using a conventional May–Giemsa staining procedure (data not shown). Next, we further sorted the two leukocyte fractions in Fig. 2D with the cell sorter and used May–Giemsa staining to reveal that the $MIL4^{-}SSC^{large}CT7^{-}$ population, the gated subpopulation in Fig. 2D, was comprised of eosinophils and basophils (Fig. 3A). However, another $MIL4^{-}SSC^{large}CT7^{high}$ population, unique to guinea pigs, generally contained an inclusion body in the cytoplasm